

2017

Pre-synaptic and post-synaptic pathways from the hippocampus to medial prefrontal cortex in Rhesus monkeys

<https://hdl.handle.net/2144/27066>

"Downloaded from OpenBU. Boston University's institutional repository."

BOSTON UNIVERSITY
SARGENT COLLEGE OF HEALTH AND REHABILITATION SCIENCES

Thesis

**PRE-SYNAPTIC AND POST-SYNAPTIC PATHWAYS
FROM THE HIPPOCAMPUS TO MEDIAL PREFRONTAL
CORTEX IN RHESUS MONKEYS**

by

IFEANYIROCHUKWU N. ONOCHIE

B.S., Rutgers University, 2013

Submitted in partial fulfillment of the
requirements for the degree of
Master of Science

2017

Approved by

First Reader

Helen Barbas, Ph.D.
Professor of Health Sciences
Boston University, Sargent College of Health and Rehabilitation
Sciences

Professor of Anatomy and Neurobiology
Boston University, School of Medicine

Second Reader

Miguel A. Garcia-Cabezas, MD, Ph.D.
Research Assistant Professor of Health Sciences

Acknowledgements

I thank my advisor, Helen Barbas, for her continuous encouragement and guidance throughout my master's work. I thank Miguel A. Garcia-Cabezas for his outstanding support and advice. I thank PhD candidate, Jingyi Wang, for her patience and teachings throughout the entirety of my work. I thank PhD candidate Mary Kate Joyce for assistance in various areas of my thesis. Finally, I thank my colleagues whom all played a large role in the success of my masters work; Iris Trutzer, Yohan John, Tara McHugh, Marcia Feinberg and Nayeem Hossain.

**PRE-SYNAPTIC AND POST-SYNAPTIC PATHWAYS
FROM THE HIPPOCAMPUS TO MEDIAL PREFRONTAL
CORTEX IN RHESUS MONKEYS
IFEANYIROCHUKWU N. ONOCHIE**

ABSTRACT

The hippocampal to medial prefrontal cortex (HPC-mPFC) pathway has a role in mnemonic processing. A key function of the hippocampus (HPC) is to organize contextual memories by how they were experienced, and the prefrontal cortex (PFC) retrieves contextual memories by sorting and suppressing irrelevant memories for the task at hand. Studies have highlighted the HPC-mPFC connection in rodents, however, there is a relative paucity of primate studies. The present study addressed this issue by investigating the connection from the HPC to anterior cingulate cortex (ACC; areas 24a, 25 and 32) of the mPFC in rhesus monkeys (*Macaca mulatta*). The distribution of hippocampal axons and terminals (boutons) was largest in area 25. Bouton diameter was largest in the deep layers of area 25, suggesting an efficient transmission system from the HPC. The robust projections from the HPC terminated most densely in the superficial layers of area 25. The HPC pathway also innervated some inhibitory neurons, labeled for the calcium binding proteins calbindin or calretinin in the superficial layers of the ACC, whereas axons innervated parvalbumin inhibitory neurons in the deep layers of the ACC. The findings suggest that area 25 may be a fundamental pathway from the HPC for memory processing

and can be a focal point in therapeutic interventions in neurological and psychiatric diseases.

TABLE OF CONTENTS

Acknowledgements	iv
Abstract	v
Table of Contents	vii
List of Tables	viii
List of Figures	ix
List of Abbreviations	xi
Introduction	1
Materials and Methods	9
Results	17
Discussion	37
References	48
Vita	57

LIST OF TABLES

TABLE 1	
Injection sites and tracers in the HPC	10
TABLE 2	
Double labeling for pathway tracers and inhibitory neurons	13
TABLE 3	
Labeled boutons circled across sites per case, layer and area: each site includes a column of cortex from pia to white matter	22
TABLE 4	
Hippocampal axons apposed to elements labeled for calcium binding proteins	34
TABLE 5	
Hippocampal axons apposed to elements labeled for calcium binding proteins, by layer	34

LIST OF FIGURES

FIGURE 1	
Axon tracing for case BT-L: HPC to mPFC	19
FIGURE 2	
Axon tracing for case BQ-L: HPC to mPFC	20
FIGURE 3	
Bouton diameter analysis	26
FIGURE 4	
Bouton diameter cluster analysis	27
FIGURE 5	
Bouton diameter analysis in large cluster	28
FIGURE 6	
Bouton distribution comparison between superficial and deep layers	30
FIGURE 7	
Density of pathway terminations in medial prefrontal areas	31
FIGURE 8	
Examples of hippocampal axons apposed to elements of inhibitory neurons in the mPFC	35
FIGURE 9	
Areal pattern of hippocampal axons apposed to elements of inhibitory neurons in the ACC	36

FIGURE 9

Laminar pattern of hippocampal axons apposed to elements of inhibitory neurons in 36
the ACC

LIST OF ABBREVIATIONS

ACC	Anterior cingulate cortex
AD	Alzheimer's disease
Alexa488	Alexa fluor 488
CA1	Cornu Ammonis 1
CA2	Cornu Ammonis 2
CA3	Cornu Ammonis 3
CB	Calbindin
CBL	Cascade blue dextran
CBPs	Calcium binding proteins
CE	Gundersen coefficient of error
CR	Calretinin
DG	Dentate gyrus
EC	Entorhinal cortex
FE	Fluoroemerald
HPC-mPFC	Hippocampal-medial prefrontal cortex
HPC	Hippocampus
mPFC	Medial prefrontal cortex
NFTs	Neurofibrillary tangles
PFC	Prefrontal cortex
PV	Parvalbumin
Re	Nucleus Reuniens

SD

Standard deviation

SE

Standard error

Introduction

The hippocampal – medial prefrontal cortex (HPC-mPFC) pathway is part of an important network involved in emotion, cognition and memory. My research focuses on the organization of this pathway, involved in memory such as episodic memory and working memory. Our brains are constantly processing information and are able to sort out important memories for specific tasks, while suppressing irrelevant information (Miller & Cohen, 2001). Working memory refers to the ability to use relevant information/memories for a task. Animal and human studies have shown that working memories are short term and necessary for these relevant tasks (Floresco *et al.*, 1997; Churchwell & Kesner, 2011). Episodic memories refer to past personal events or experiences that include contextual details of those events (Jin & Maren, 2015). Years of research have shown that the hippocampus (HPC) and medial prefrontal cortex (mPFC) connection is essential for retrieval and encoding of episodic memories (Kennedy & Shapiro, 2004; Hasselmo & Eichenbaum, 2005; Preston & Eichenbaum, 2013).

Several rodent studies have been conducted on the HPC, however there is a shortage of primate research in the HPC and its interaction with the mPFC (Squire, 1992; Aggleton & Brown, 1999; Simons & Spiers, 2003). The primate HPC is larger in size and is more intricate in comparison to rodents. Specifically, the CA1 of the HPC is more diverse in primates in regards to cytoarchitecture (Rosene & Van Hoesen, 1987). The primate cortex is more closely related to humans with regard to both structure and function and has been a widely used animal model to study high order brain function

(Orban *et al.*, 2004; Barbas & Zikopoulos, 2006; Barbas *et al.*, 2011). Therefore, the animal model used in my research is the rhesus monkey (*Macaca mulatta*).

While there are only a few studies involving the primate HPC-mPFC connection, there have been significant findings (Barbas & Blatt, 1995; Insausti & Munoz, 2001; Aggleton *et al.*, 2015). Among these findings, some were obtained by using retrograde tracers, which label pathways backwards, from the termination site to cell body. These tracers are placed in various architectonic areas of the prefrontal cortex (PFC) and did not allow analysis of specific terminations from the HPC to the PFC. The present study used anterograde tracers, which label pathways from the cell body to the termination site of axons. This method allowed for an in-depth look at the terminations of pathways from the HPC to the mPFC and their laminar distribution. By characterizing this pathway involved in memory, we can also get further insight of possible involvement of this pathway in Alzheimer's disease (AD), a neurodegenerative disease, and psychiatric disorders such as schizophrenia and post-traumatic stress disorder. Thus, the connection between the HPC and the mPFC can be a specific target for therapeutic drugs/interventions for these diseases.

The Hippocampus: structure involved in memory processing

The HPC is located in the medial temporal lobe and is part of the limbic system. The key function of the HPC is to organize contextual memories, which is a feature of episodic memory (Eichenbaum, 2017). It is characterized by its unidirectional pathways, both functionally and anatomically, as well as laminar distinctions. The primate HPC

consists of the Cornu Ammonis fields (CA1-CA3), the subicular complex and the dentate gyrus (DG) (Insausti & Munoz, 2001). The DG and hippocampal proper are heavily involved in processing information that travels through the HPC, which coordinates and sorts information from various inputs (Amaral *et al.*, 2007). The HPC has a rare capability for adult neurogenesis (creation of new neurons) that can develop and seamlessly adapt into already existing neural paths (Anacker & Hen, 2017).

The HPC has been widely studied as a structure associated with memory retrieval, encoding and storage (Barbas *et al.*, 1999; Insausti & Munoz, 2001; Ranganath *et al.*, 2005). One of the first studies to highlight the importance of the hippocampal formation in memory involved patient Henry Molaison (H.M.), and this case was fundamental in the advancement in memory research (Scoville, 1954; 1957; Penfield & Milner, 1958; Blatt & Rosene, 1998; Squire & Wixted, 2011). H.M. was knocked over in a bicycle accident and started to have seizures that progressively worsened as he got older. By his mid-teens he was having severe seizures (Squire & Wixted, 2011). Drugs could not treat his seizures, so he had a bilateral medial temporal lobectomy in hopes of helping his epilepsy. After this surgery, H.M. suffered from anterograde amnesia, which is the inability to form and store new memories (Scoville & Milner, 1957). The H.M. case gave insight as to how medial temporal lesions affected his memory during certain tasks. Ultimately, animal models began using tasks solely affected by medial temporal lesions (Mishkin, 1978; Squire & Wixted, 2011). The present study on rhesus monkeys will provide information on the specific pathway from the HPC to the mPFC that affects memory.

Evidence also shows that the HPC is important for forming new declarative memories (Squire *et al.*, 2004). This was concluded based on the lesion studies of H.M. and the vast number of cortical areas that project to the HPC. During encoding, a scenario is processed in several association areas and the HPC then takes these processed memories and bring them together to form a declarative memory (Howard *et al.*, 2005; Ranganath *et al.*, 2005). Activation of the HPC also occurs during navigational tasks and spatial memory in both humans and animals (Eichenbaum, 2017).

The HPC has three, unidirectional pathways that direct the flow of information (Amaral, 1993; Ongur & Price, 2000). The first pathway involves entorhinal cortex axons that project to the DG. The projections from the DG are sent to CA3 pyramidal cells through mossy fibers. Information is then communicated by the CA3 neurons to CA1 pyramidal neurons through Schaffer collaterals. These pyramidal neurons project to the deep layers of the entorhinal cortex (EC). The second pathway differs by the EC sending direct projections to CA3 instead of through the DG. Finally, in the third pathway, CA1 receives direct projections from layer III of the EC (Rosene & Van Hoesen, 1977; Cenquizca & Swanson, 2007).

The anterior cingulate cortex of the mPFC receives strong projection from the HPC

The PFC is a very complex region that makes up the rostral half of the frontal lobe. It consists of the orbital, medial and lateral areas that are directly anterior to premotor areas in the caudal half of the frontal cortex (Barbas, 1995). The PFC plays a pivotal role in orchestrating cognitive control throughout the cortex (Miller & Cohen, 2001). Another key function of the PFC is to retrieve contextual memories by sorting and suppressing context inappropriate memories (Eichenbaum, 2017). It is a complex region in primates, in behavior and function. In rodents, the PFC is smaller and comparatively underdeveloped. There is a relative paucity of primate research in the mPFC in comparison to human and rat studies. While non-human primates do not exhibit identical architectonic areas, they are more closely related to humans than rodents. The PFC sends out signals to almost all premotor, sensory and high order association cortices (Barbas, 1995; 2015). Therefore, even the most basic behavior requires intricate interactions between the input and output systems of the PFC.

The medial portion of the PFC has many distinct areas found above and below the rostral part of the corpus callosum. The mPFC has connections with limbic structures such as perirhinal, entorhinal, cingulate cortices, the amygdala and HPC (Van Hoesen *et al.*, 1975; Rosene & Van Hoesen, 1977; Amaral & Price, 1984; Insausti *et al.*, 1987; Barbas & De Olmos, 1990; Morecraft & Van Hoesen, 1992). Areas 24a, 25 and 32 are caudal areas of the mPFC, which exhibit similarities in structure and function (Barbas *et al.*, 1999). These areas are collectively termed the anterior cingulate cortex (ACC). The

ACC is dysgranular (exhibits a poorly developed layer IV) or agranular (lacking layer IV) and show evidence of having prominent deep layers (Barbas & Pandya, 1989; Insausti & Amaral, 2008). Area 24a is the inner part of area 24 in the ACC. It lacks a granular layer IV and layer IIIb pyramidal cells merge with layer V. Area 32 of the ACC has dense connections with the PFC (Barbas & Pandya, 1989) and area 25 has dense connections with the amygdala and the HPC (Barbas & Blatt, 1995; Carmichael & Price, 1995; Insausti & Munoz, 2001; Ghashghaei *et al.*, 2007). The ACC in its entirety receives the strongest projections from the CA1 of the HPC among prefrontal areas (Barbas & Blatt, 1995).

Studies have more recently recognized the mPFC as playing an integral role in memory, due to the robust projections from the HPC. The mPFC is involved in fear recollection in rodents (Corcoran & Quirk, 2007), reward learning (Rushworth *et al.*, 2011) and memory consolidation (Tronel & Sara, 2002). Multiple studies have highlighted the role of the mPFC in regards to memory, suggesting that lesions to this area may result in memory-based impairments (Sigurdsson *et al.*, 2010; Hembrook *et al.*, 2012; Godsil *et al.*, 2013; Navawongse & Eichenbaum, 2013; Preston & Eichenbaum, 2013). Evidence suggests that the mPFC is important in retrieving contextual episodic memories in the HPC (Preston & Eichenbaum, 2013).

The HPC-mPFC pathway plays a key role in mnemonic processing

Although the physiology of this pathway had been studied widely in rodents, some of the more dense projections from CA1 to mPFC are seen in primates (Zhong *et al.*, 2006). Direct cortical output from the CA1 to the frontal lobe has been found in several studies (Vogt & Pandya, 1987; Barbas & Blatt, 1995; Carmichael & Price, 1995; Insausti & Munoz, 2001). The projections from the CA1 to the mPFC in primates suggest a role in memory encoding and retrieval (Morecraft *et al.*, 1992; Barbas *et al.*, 1999; Insausti & Munoz, 2001; Preston & Eichenbaum, 2013; Aggleton *et al.*, 2015; Jin & Maren, 2015). With advancement in technology, neuroimaging studies have provided further insight on this pathway.

The mPFC has various connections to different cortical areas that extend to the HPC (Eichenbaum, 2017). There are two pathways connecting the HPC and mPFC, involving a thalamic route and a cortical route (Eichenbaum, 2017). In the thalamic route, mPFC areas and the nucleus reuniens (Re), which is thought to synchronize the HPC and mPFC (Cassel *et al.*, 2013; Mitchell *et al.*, 2014), are connected through bidirectional pathways. Bidirectional connections between the Re and CA1 have also been discovered (Dolleman-Van der Weel *et al.*, 1997; Vertes, 2006). The mPFC has strong connections with the deep layers of the lateral entorhinal cortex and the superficial layers of the perirhinal cortex, and both are connected with the HPC (Burwell & Amaral, 1998; Witter *et al.*, 2000; Eichenbaum, 2017). Both the lateral entorhinal and perirhinal cortices are

involved in providing relevant information for behavioral actions and objects (Igarashi *et al.*, 2014; Keene *et al.*, 2016).

In human and animal studies, the HPC and the mPFC were shown to both activate when memory tasks are performed (Preston & Eichenbaum, 2013; Sigurdsson & Duvarci, 2015). The extent of the sites activated heavily depended on the specific task and was shown that specific pathways were activated during encoding versus retrieval of memories (Henson *et al.*, 1999). Interestingly, the amount of activation during these tasks can determine how much memory is stored.

The HPC and mPFC in rodents have been shown to synchronize in rhythmic activity of neurons during spatial working memory tasks (Jones & Wilson, 2005; Sotres-Bayon *et al.*, 2012; Giustino & Maren, 2015). This finding provides evidence that there is indeed interaction between these two structures in regards to memory. Studies have also explored the projections from the pathway and discovered that these projections are glutamatergic pyramidal neurons that terminate on principal or GABAergic neurons in the mPFC (Tierney *et al.*, 2004). Additional lesion studies involving this pathway would provide further information about how the connection is involved in memory.

Additional studies of the HPC and mPFC are necessary in primates to help understand their role in memory and the consequences of disruption in this pathway. This pathway is exceptionally sensitive to stress, which is a key factor in many disorders (Godsil *et al.*, 2013). This may help explain why several neurodegenerative diseases and psychiatric disorders have been linked to these structures and their connections (Liberzon

& Sripatha, 2008; Godsil *et al.*, 2013). By understanding this connection, there is a potential for an alternate route for memory processing when dealing with diseases, such as AD, in which the entorhinal cortex is affected early in the disease (Gomez-Isla *et al.*, 1996). I aim to further characterize the pathway from the HPC to mPFC in rhesus monkeys. This research is needed to understand the pathway in primates, which are more closely related to humans than rodents.

Materials and Methods

Experimental design

The experimental design is based on injections of anterograde neural tracers into the CA1 of the HPC in rhesus monkeys. This approach labels the pathway connection between the HPC and ACC of the mPFC. The first goal was to investigate axonal and bouton distribution to give a comprehensive map on their laminar distribution in the ACC of the mPFC. Information gathered from the neural tracers include bouton diameter per area and layer, as well as bouton density.

Another goal was to study the organization of hippocampal pathways to the mPFC, as they innervate excitatory and some inhibitory neurons in ACC areas 24a, 25 and 32. The pathways in the cortex are excitatory and mostly innervate excitatory neurons. However, about 20-30% of axon terminals innervate inhibitory neurons. I double labeled for calcium binding proteins Calbindin (CB), Calretinin (CR), and

Parvalbumin (PV), which label distinct classes of inhibitory neurons in primates and used laser scanning confocal microscopy to study appositions between hippocampal axons and inhibitory neurons in the ACC. The goal was to study whether axon terminations in the mPFC formed appositions with inhibitory neurons. This is when a labeled dendrite of a post-synaptic neuron and an axon terminal make contact with one another. This will provide insight on how the pathway innervates specific classes of inhibitory neurons in particular areas and layers of the ACC.

Surgery and neural tracer injections

Experiments were conducted on rhesus monkey cases (n = 4), all female, aged 3 to 4 years old. All injection sites of tracers were in the CA1 of the HPC and three different neural tracers were used (Table 1). Experiments were conducted using the Guide for the Care and Use of Laboratory Animals and were approved by the institutional animal care and use committees at Boston University School of medicine, Harvard Medical School, and New England Primate Research Center.

Table 1: Injection sites and tracers in the HPC

Case	Hemisphere	Age (years)	Sex	Tracer/Dye
BQ	left	3.5	Female	Alexa 488 (10K)
BT	left	4	Female	FE (10K + 3K)
BS	right	3.5	Female	CBL (10K + 3K)
BU	left	3	Female	CBL (10K + 3K)

Magnetic resonance images were taken to obtain stereotaxic coordinates before surgery, following sedation with ketamine hydrochloride and propofol anesthesia. Stereotaxic coordinates are needed to drive the needle for injection of neural tracers to the desired injection site. Animals were monitored consistently for temperature, heart rate, respiratory rate, oxygen saturation, etc. and the experiments were conducted under sterile conditions. For the surgery, animals were sedated and then anesthetized and placed in a stereotaxic apparatus and a small hole in the dura and skull was made. Ten percent dilutions of fluoroemerald (FE, cocktail of 10K and 3K), Alexa fluor 488 (Alexa 488, 10K) or cascade blue dextran (CBL, cocktail of 10K and 3K) were injected into the HPC.

Perfusion and tissue processing

After 20-23 days to allow for tracer transport, animals were given an overdose of anesthesia with sodium pentobarbital, and perfused with 0.2% glutaraldehyde in 0.1 M PBS (phosphate buffer saline) and 4% paraformaldehyde (20 days for case BQ and BS, 21 days for case BT and 23 days for case BU). The brain was then removed and cryoprotected using ascending sucrose solutions (10-25% sucrose in 0.1 M PBS with 0.05% sodium azide). Shortly after, the brain was frozen in isopentane at -80°C and cut using a freezing microtome (AO Scientific Instruments, Reichert Technologies). The slices were coronal sections, 50 µm thick and cut in 10 matched series. The cut sections were then stored at -20°C in a cryoprotection solution (0.05% sodium azide, 30% ethylene glycol and 30% glycerol).

Labeling of pathways and inhibitory neurons

Immunohistochemistry was conducted in all cases listed in Table 1. Free floating tissue sections were rinsed with 0.01M PBS at 4°C. For antigen retrieval to help view signal, 10 mM sodium citrate buffer was used. The 10 mM sodium citrate buffer is made with 2.94g Tri-sodium citrate and 1000 ml dH₂O, and PH to 8.5. A dH₂O water bath is heated to 80°C with the purpose of slowly bringing the sodium citrate to that temperature. The tissue was incubated in 80°C antigen retrieval buffer for 30 minutes and cooled 30 minutes to room temperature on a room temperature shaker. A second rinse was conducted with 0.01M PBS at 4°C. The tissue was then incubated in 50mM of Glycine at 4°C for 1 hour. Pre-block buffer stock solution and primary/secondary antibody buffer solution were made with 0.1 M PB, 10% Bovine Serum Albumin, 0.2% BSA-C, 10% Normal goat serum, 0.2% Triton X-100. A third rinse was completed and the tissue was incubated in the pre-block solution at 4°C for 1 hour. To investigate hippocampal terminations on inhibitory neurons in the mPFC, I double labeled sections for the calcium binding proteins CB, CR and PV to label inhibitory neurons, along with pathways labeled with a tracer (Table 2).

Table 2: Double labeling for pathway tracers and inhibitory neurons

Case	Primary antibody for tracers	Tracer converted for fluorescence (wavelength)	Primary antibody for calcium binding proteins	Calcium binding proteins converted for fluorescence (wavelength)
BQ-L	RbtAlexa488	405	MseCB/CR/PV	647
BT-L	RbtFE	488	MseCB/CR/PV	647
BS-R	RbtCBL	405	MseCB/CR/PV	647
BU-L	RbtCBL	488	MseCB/CR/PV	647

Tissue sections were then incubated with primary antibodies for tracers (rabbit FE, rabbit CBL, and rabbit Alexa488: 1:800 in primary antibody buffer solution) and calcium-binding proteins (mouse CB, mouse CR, and mouse PV: 1:2000 in primary antibody buffer solution) for three days. Each day, the tissue was microwaved at 150W for 8 minutes in 4 degrees (3 minutes on, 2 minutes off, 3 minutes on). On the third day we rinsed the tissue with 0.01 M PBS buffer and then incubated the tissue in secondary antibodies conjugated with fluorescent label overnight at 4°C (Alexa 488 goat anti-rabbit IgG or Alexa 405 goat anti-rabbit: 1:100 and Alexa 647 goat anti-mouse: 1:100 all in secondary antibody buffer solution), including a microwave process at 150W for 8 minutes in 4°C. The tissues was then rinsed with 0.01 M PBS, pH 7.4 and mounted on slides. Tissues were left to dry for 2 days and cover slipped with Prolong Gold Antifade mounting solution (Invitrogen).

Distribution of axons from the HPC to mPFC

Axon mapping was used to investigate the area and laminar distribution patterns, regarding the projection between the HPC to mPFC (areas 24a, 25 and 32). The program used for axon mapping was the Neurolucida (MicroBrightField). Cases BT-L and BQ-L, half series (1 section/mm), were used for axon mapping. For each tissue section in both cases, boundaries were drawn for all three areas and layers at 25X magnification. After boundaries were completed, axons were traced within these set boundaries at 400X magnification. This method allowed for a comprehensive map of axon distribution and comparison between the superficial and deep layers. It also gave a clear view of which areas were denser with regards to axon distribution from the HPC.

Major diameter of hippocampal boutons in the ACC

Multiple sections, anterior to posterior, of each case were photographed at 20X magnification (Olympus BX 51 light microscope) in order to determine boundaries of areas 24a, 25 and 32 in the PFC and all layers. Area 24a is agranular (lacking a layer IV) and areas 25 and 32 are dysgranular, which indicates that layer 4 is poorly formed in these cortical areas. Laminar distinction is quite poor in these areas (Barbas & Pandya, 1989). Once boundaries were determined, 20 images were taken throughout the thickness of the section and boutons were captured at 1000X magnification to analyze the size of hippocampal axon terminals in the ACC. A comparable number of images were taken per case. Columns of cortex from 3-4 sites were acquired, per case and per area. Using Image J (NIH, USA), these images were combined into stacks to create one merged image.

Labeled boutons in the ACC were traced manually using the program Reconstruct (Fiala, 2005) (n = 45,549). Data were exported to a database in Windows Excel. Using Matlab, I used k-means cluster analysis to separate boutons into small and large clusters, by determining a cutoff point of the bouton diameter.

The diameter distribution was acquired by grouping boutons under certain diameters (<0.2, <0.4, <0.6, etc.) and by finding the percent distribution of those boutons in each area (area 24a, 25 and 32) and layers. Data were then grouped into superficial layers (layer I-III) and deep layers (layers V-VI) for analysis as well as small and large clusters.

Distribution and density of boutons from the HPC to MPFC: Stereological methods

I used unbiased systematic stereological analysis to determine overall bouton distribution in areas 24, 25 and 32, as well as between layers. The program used to randomly sample areas for this study was Stereo Investigator. The Optical Fractionator uses systematic random sampling (SRS) to select a sample from each area of the mPFC in an unbiased manner at constant intervals (Glaser & Wilson, 1998). Boutons were counted and the system provided an accurate estimate of the number of boutons within the areas of interest.

The disector, which is the cell counting frame size, was set at 60 μm x 60 μm . The grid layout indicated how many random samplings would be needed per area and layer, which was determined after a pilot study. For case BT-L, the grid was 1000 x 1000

for area 25, 100 x 100 for area 24a and 250 x 250 for area 32. For case BQ-L, the grid layout was 800 x 800 for area 25, 500 x 500 for area 24a and 500 x 500 for area 32. Both BT-L and BQ-L were half series (1 section/mm). Sampling was done at the microscope at 1000X magnification.

After random sampling was complete, I assessed the sampling results provided by Stereoinvestigator to see if the Gundersen coefficient of error (CE), $m=1$, was met across cases, areas and layers (Gundersen *et al.*, 1999). The CE, which should have a value of 10% (.1) or less, is used to estimate the accuracy of a population size estimate. While there are several types of coefficients of error that can be used for stereology, the Gundersen error is used when three or more sections are randomly sampled (Gundersen *et al.*, 1999).

Relationship of hippocampal pathways to inhibitory neurons

To study potential appositions between hippocampal axons targeting inhibitory neurons in the mPFC, inhibitory neurons were labeled for the calcium binding proteins, CB, CR and PV. I used a laser scanning confocal microscope (Fluoview FV-300, Olympus; LSM-510, Carl Zeiss Microscopy). Labeled fibers in cortical layers were captured for each case in all areas in the superficial and deep layers. The stacks of each section were acquired and then processed in Zen 2.3 (Blue) Lite. Zen Blue is used for image acquisition, processing and analysis by saving several stacks of images (z-stacks) from all positions into one file. Next, AutoDeblur and AutoVisualize, an image deconvolution software, was used to remove blurry scatter from the confocal images.

Finally, Image J and Reconstruct were used to detect and count all appositions between the hippocampal axon and elements of inhibitory neurons. These programs allowed me to look through the thickness of the sections for any appositions, and provided a 3D view of hippocampal axons apposed to inhibitory neurons in the mPFC. This 3D view is pivotal for accurate detection of appositions.

Results

Injections sites in the HPC

The pathways labeled with neural tracers are indicated in Table 1. The injection sites for all cases were situated in the CA1 of the HPC. Studies have shown that the areas with the highest density of projection neurons to the mPFC from the HPC originate in the CA1 in rodents (Jay & Witter, 1991; Cenquizca & Swanson, 2007) and primates (Barbas & Blatt, 1995; Insausti & Munoz, 2001).

Hippocampal axons preferentially target superficial layers of anterior area 25 and deep layers of posterior area 25

I mapped labeled axons from the HPC to the mPFC (cases BT-L and BQ-L) and comprehensive maps using axon tracing (Figures 1-2) showed that area 25 had a larger number of axon terminals compared to areas 24a and 32. In both cases, the more posterior coronal sections of the series had higher axon density, while axons in the more

anterior coronal sections were comparatively sparse. Both cases exhibited this trend. Further analysis revealed that the posterior sections in both cases had the highest axon density in the deep layers. As we move through more anterior levels in the series, higher axon density is seen in the superficial layers. Previous research indicated that labeling was most prevalent in layer III (Aggleton *et al.*, 2015). Producing an axonal tracing map allowed me to see that the results are consistent with previous findings.

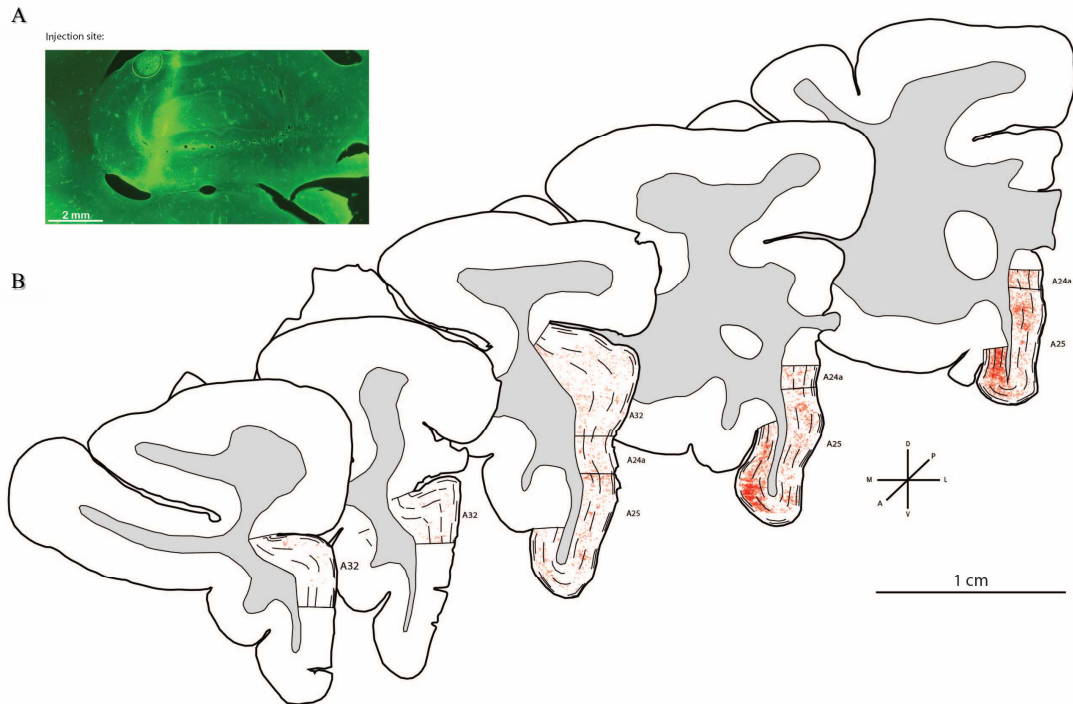


Figure 1: Axon tracing for case BT-L: HPC to mPFC. Axon mapping of pathways from the HPC to mPFC (case BT-L). **A.** Injection site in the CA1 of the HPC with tracer Alexa488 (10K); Scale: 2.0 mm **B.** Sections from anterior to posterior (left to right). Axons were mapped (red) in the mPFC (Area 24a, A25 and A32). Axons were sparse in the anterior sections of this case, and increased in density more posteriorly. Scale: 1 cm, White matter is shown in grey.

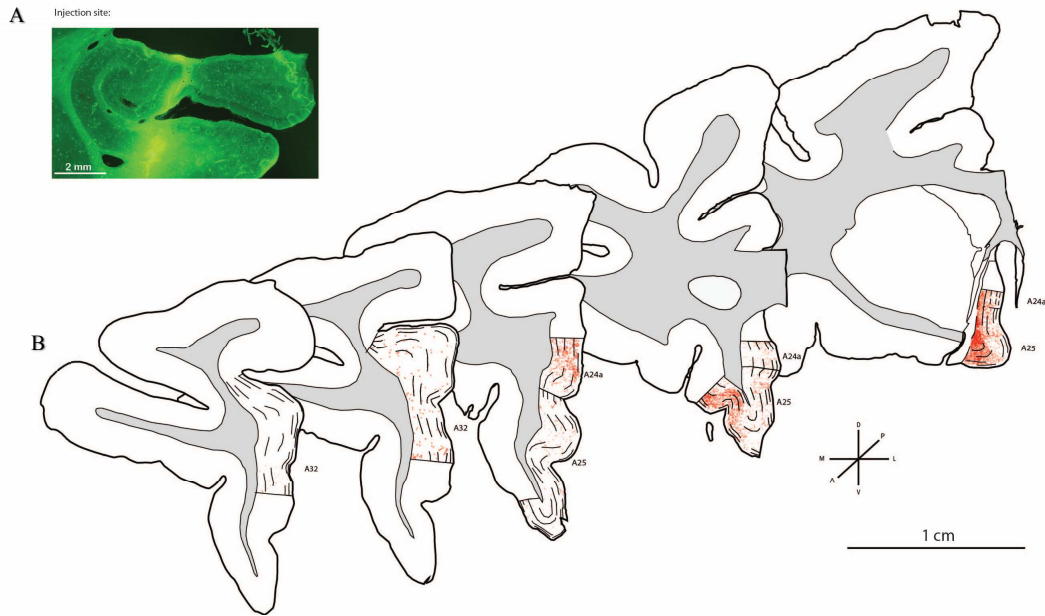


Figure 2: Axon tracing for case BQ-L: HPC to mPFC. Axon mapping of pathways from the HPC to mPFC (case BQ-L). **A.** Injection site in the CA1 of the HPC with tracer FE (10K + 3K); Scale: 2.0 mm **B.** Sections from anterior to posterior (left to right). Axons were traced/mapped (red) in the mPFC (Area 24a, A25 and A32). Axons were sparse in the anterior sections of this case (left), and increased in density more posteriorly (right). Scale: 1 cm, White matter is shown in grey.

Large boutons in area 25 may represent increased synaptic efficiency

To study bouton diameter, I first manually circled boutons using Reconstruct in all areas from all cases (n = 4 cases; 45,549 boutons). This process showed that area 25 had the largest number of boutons in comparison to areas 24a and 32 of the mPFC (Table 3). I then examined the major diameter of the boutons previously circled. When the diameter of the bouton is large, there is also a possibility for more mitochondria and synaptic vesicles to be present (Zikopoulos & Barbas, 2006; 2007a; b; García-Cabezas & Barbas, 2016). A larger number of synaptic vesicles may result in an increase in neurotransmitter released and facilitate signal transmission (Tong & Jahr, 1994; Frerking & Wilson, 1996; Murthy *et al.*, 1997). The size of the bouton may also determine what type of role a certain pathway will have on activity on the projection site. Larger boutons likely have a “driver” role that could potentially elicit activity in the mPFC and smaller boutons may be modulatory to the system (Barbas *et al.*, 2013).

Table 3: Labeled boutons circled across sites per case, layer and area: each site includes a column of cortex from pia to white matter

A. Case BQ-L

	Area 24a		Area 25		Area 32	
	Number of sites	Number of boutons per layer	Number of sites	Number of boutons per layer	Number of sites	Number of boutons per layer
Layer I	4	38	3	52	3	0
Layer II	4	1,951	4	936	4	301
Layer III	4	661	4	788	4	805
Layer V	4	994	4	1,068	4	902
Layer VI	4	835	4	1,652	4	1,404
Total	20	4,479	19	4,496	19	3,412

Case BT-L

	Area 24a		Area 25		Area 32	
	Number of sites	Number of boutons per layer	Number of sites	Number of boutons per layer	Number of sites	Number of boutons per layer
Layer I	3	0	4	17	3	0
Layer II	4	735	4	509	4	694
Layer III	4	1,452	4	1,587	4	750
Layer V	4	2,173	4	2,466	4	874
Layer VI	4	1,010	4	1,035	4	1,188
Total	19	5,370	20	5,614	19	3,506

Case BU-L

	Area 24a		Area 25		Area 32	
	Number of sites	Number of boutons per layer	Number of sites	Number of boutons per layer	Number of sites	Number of boutons per layer
Layer I	3	0	3	0	3	0
Layer II	4	294	4	1,908	4	410
Layer III	4	237	4	1,999	4	284
Layer V	4	519	4	3,453	4	139
Layer VI	4	602	4	3,310	4	396
Total	19	1,652	19	10,670	19	1,229

Case BS-R

	Area 24a		Area 25		Area 32	
	Number of sites	Number of boutons per layer	Number of sites	Number of boutons per layer	Number of sites	Number of boutons per layer
Layer I	3	0	3	0	3	0
Layer II	4	51	4	183	4	271
Layer III	4	132	4	377	4	517
Layer V	4	398	4	482	4	1,128
Layer VI	4	484	4	450	4	561
Total	19	1,065	19	1,582	19	2,474

Total (n): 45,549

B. Total number of boutons per area

Area	Total number of boutons
24a	12,566
25	22,362
32	10,621

To further investigate bouton diameter, I compared the distribution in areas 24a, 25 and 32, as well as between superficial and deep layers. When comparing bouton diameter across the three areas, there was a consistent trend throughout the layers in each area. Figure 3A shows bouton diameter in layers I-VI and reveals that after the size of .6 μm , there is a steady decrease in the bouton distribution percentage as the diameter increases. Area 24a had the most drastic decrease in bouton distribution as size increased, whereas areas 25 and 32 had similar steady patterns. At bouton diameter of about .8 μm , area 25 had a larger percentage of boutons compared to areas 24a and 32. Furthermore, bouton diameter cluster analysis (Figure 4) revealed that area 25 had boutons with the largest diameter in both the cluster of small and large boutons, with a cutoff point of about .8 μm (small cluster: $<.8 \mu\text{m}$, large cluster $\geq .8 \mu\text{m}$).

To examine the laminar distribution in bouton diameter, the superficial layers were compared to the deep layers, as shown in Figure 3B-C. The superficial layers included layers II and III (excluding layer I). In the superficial layers, the percentage of large boutons was slightly higher in area 25, followed closely by area 32. However, the most substantial differences in bouton diameter were seen in the deep layers. Area 25 showed a higher percent of large boutons in the deep layers compared to areas 24a and 32. The proportion of boutons that had a diameter of 1 μm in area 25 was around 25%, but for areas 24a and 32, it was 10 to 15%. Cluster analysis of the deep layers (Figure 4C) showed that within the large cluster, area 25 boutons have a significantly larger bouton

diameter. By comparison, area 25 boutons represented in the small cluster did not show as drastic of a diameter difference when compared to the other areas (Figure 4C).

I then examined the area and laminar distribution amongst boutons solely within the large clusters (Figure 5). Figure 5A shows bouton diameter distribution in all layers and shows that area 25 had the largest distribution of large boutons. To further break down the laminar comparison, the superficial and deep layers were compared. It is clear that the deep layers had the highest percent distribution in the large diameter cluster.

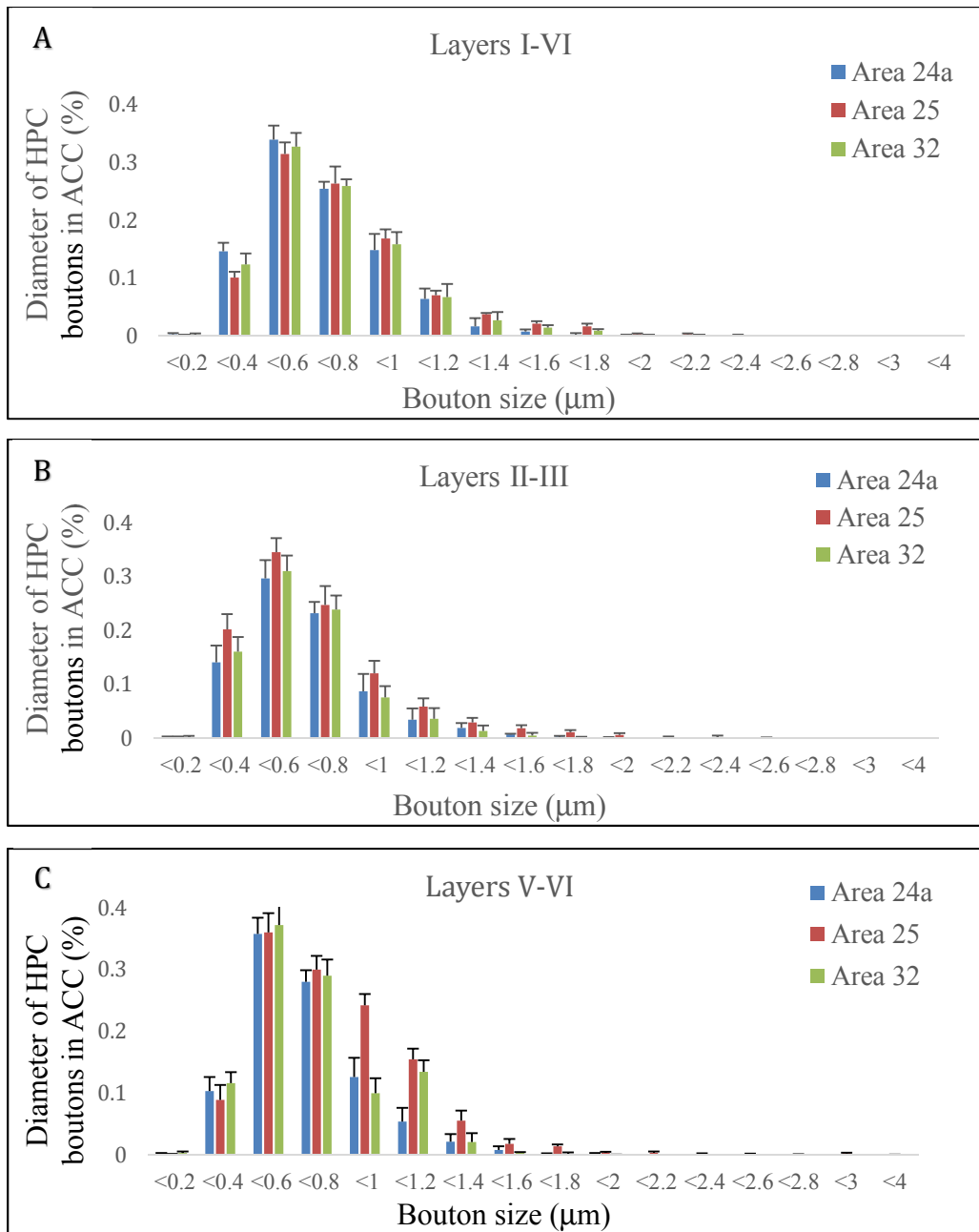


Figure 3: Bouton diameter analysis. Boutons in area 25 were larger than boutons in areas 32 and 24a. **A**, Histogram shows the percent of boutons by major diameter through all layers (I-VI), in area 24a (blue), area 25 (red) and area 32 (green). **B**, Histogram shows the percent of boutons by major diameter in layers II-III, in area 24a, area 25 and area 32. **C**, Histogram shows the percent of boutons by major diameter in layers V-VI, in area 24a, area 25 and area 32. Vertical lines indicate standard error (SE).

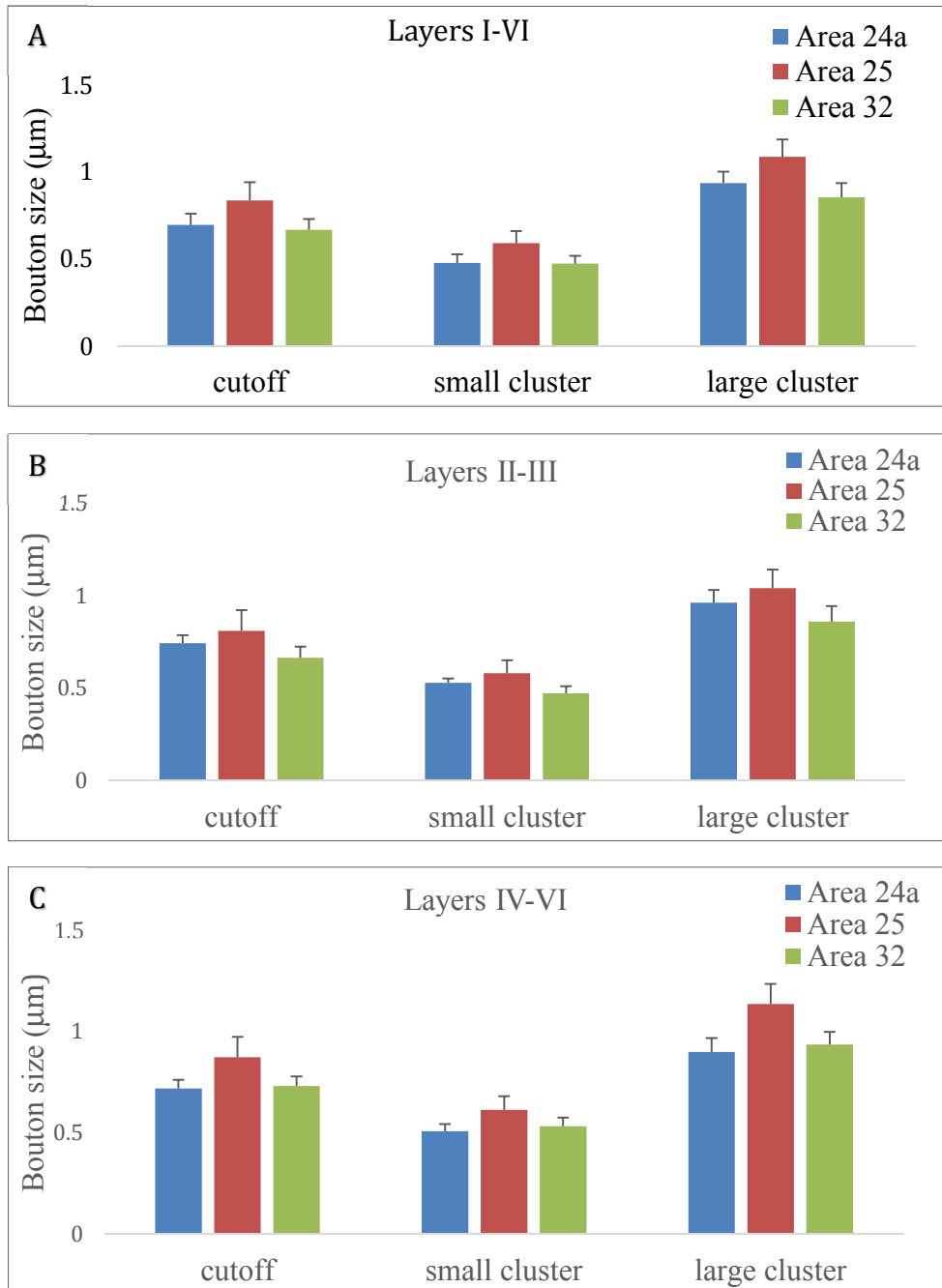


Figure 4: Bouton diameter cluster analysis. Boutons in area 25 were larger than boutons in areas 32 and 24a. **A**, Histogram shows cluster analysis for bouton diameter across all layers, in area 24a (blue), area 25 (red) and area 32 (green). **B**, Histogram shows cluster analysis for bouton diameter in layers II-III, in area 24a, area 25 and area 32. **C**, Histogram shows cluster analysis for bouton diameter in layers V-VI, in area 24a, area 25 and area 32. Vertical lines indicates SE.

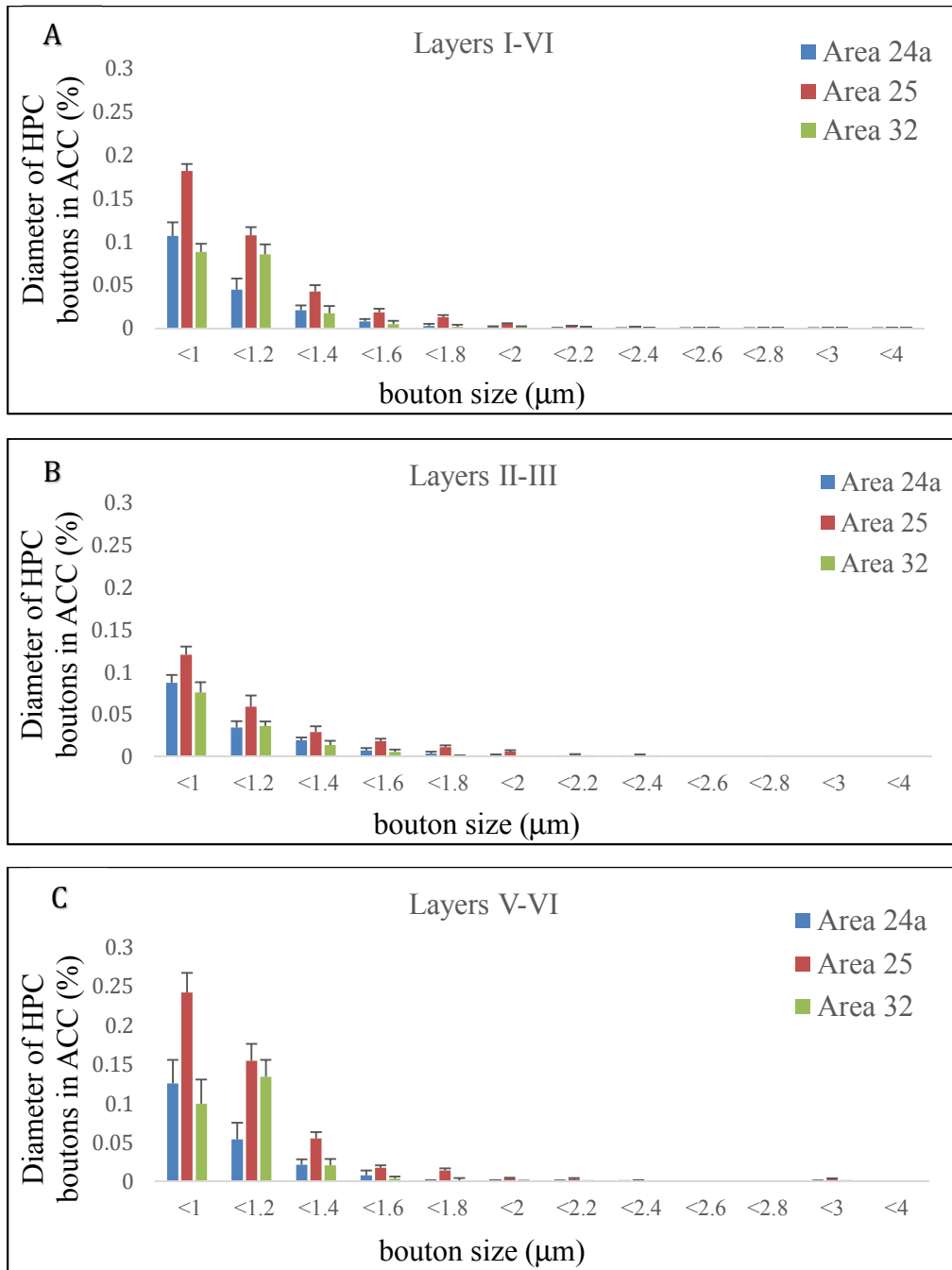


Figure 5: Bouton diameter analysis in large cluster. Bouton diameter in the large cluster shows that Area 25 (red) has a significantly larger percent bouton distribution than Area 24a (blue) and A32 (green). **A**, Histogram shows the comparison among areas and in all layers. **B**, represents the large cluster bouton diameter in the superficial layers and **C**, shows the deep layers. Vertical lines indicates SE.

Stereological analysis reveals that area 25 had a larger distribution of boutons

To obtain an unbiased analysis of bouton distribution in areas 24a, 25 and 32, as well as in different layers, stereology was conducted. First, I studied bouton distribution by comparing the mPFC areas and found that area 25 had a larger proportion of hippocampal axon terminations in comparison to areas 24a and 32. As indicated in Figure 6A, in the random samplings from the mPFC, in case BT-L 92% of boutons were found in area 25, 5% in area 32 and 3% in area 24a. These differences in proportions indicate a robust pathway from the HPC to A25. In case BQ-L, the proportion of hippocampal terminations in area 25 was lower (69%), and the rest were found in area 24a (17%) and area 32 (14%).

Next I conducted an unbiased analysis on the laminar distribution of boutons. Figure 6B shows the proportion of boutons within the superficial layers and analysis showed that area 25 had the highest average proportion of boutons. Analysis of the deep layer bouton distribution (Figure 6C) showed that area 32 had the highest proportion of boutons, however, there was a more even distribution of boutons across areas. These findings suggest area 25 plays an important role in the HPC-mPFC pathway, consistent with other findings. For example, bouton counting revealed that area 25 had the largest total number of boutons in the mPFC and bouton diameter analysis showed that area 25 had the largest proportion of boutons among the small and large clusters.

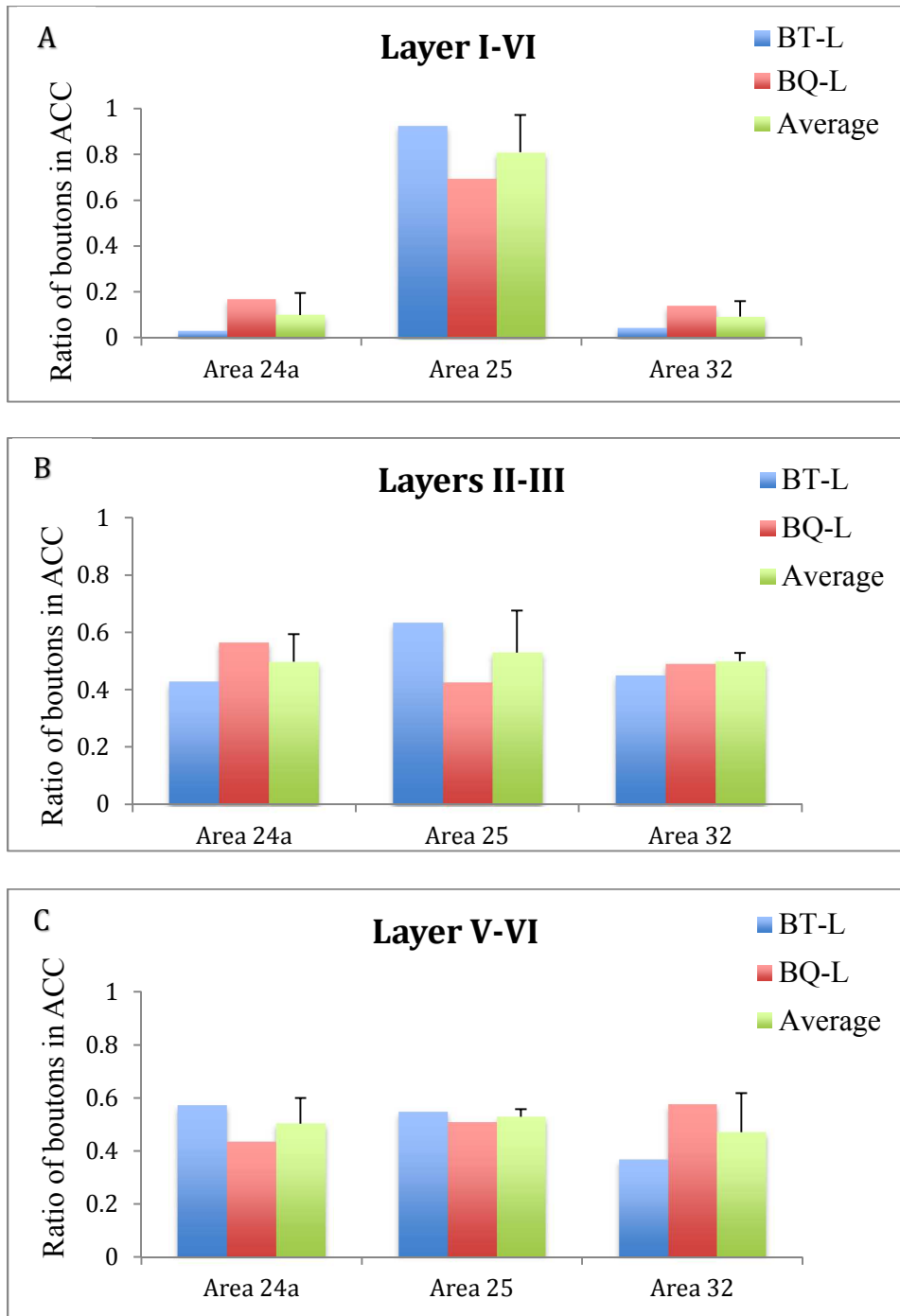


Figure 6: Bouton distribution comparison between superficial and deep layers. Bouton distribution from hippocampal axons in mPFC. **A**, Histogram shows ratio of boutons throughout the areas of interest in the mPFC. **B**, Histogram shows the ratio of bouton distributed within the superficial layer. BT-L (blue) and BQ-L (red), average (green). **C**, histogram shows the ratio of boutons within the deep layers. Vertical lines indicate standard deviation (SD).

Density of pathway terminations in ACC highest in the superficial layers of the ACC

Stereology allowed for an unbiased calculation of bouton density in the mPFC (Figure 7). Analysis revealed that A25 had the highest bouton density in both cases, in the superficial and deep layers, consistent with the analysis of labeled boutons for laminar distribution (above). Using unbiased stereology, the data showed that the superficial layers had the largest density among areas of the mPFC. These findings are consistent with the axonal maps shown in Figures 1-2.

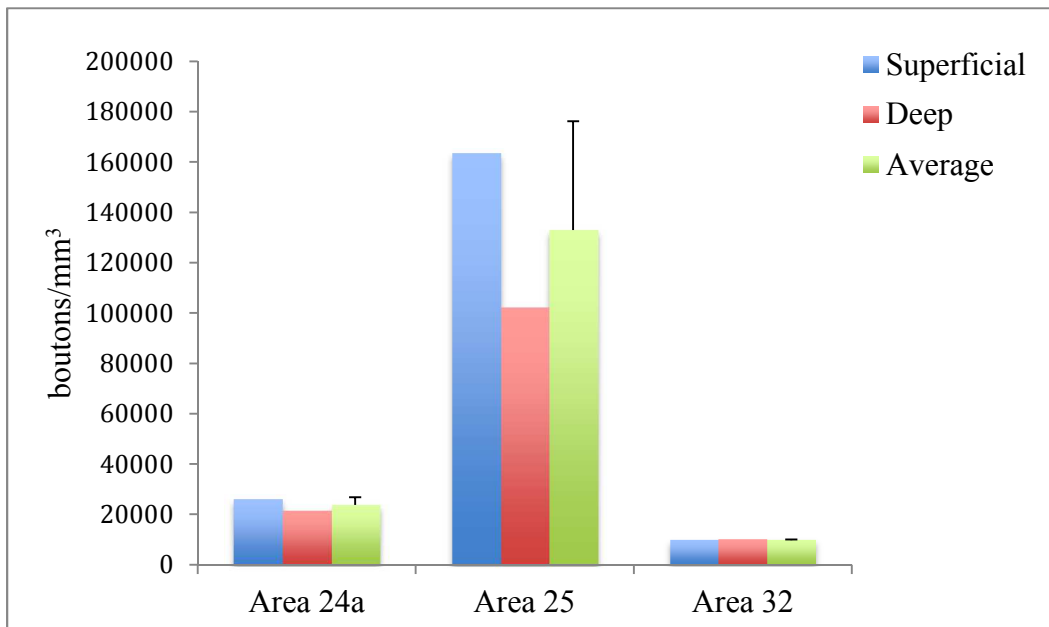


Figure 7: Density of pathway terminations in medial prefrontal areas. Pathway terminations of hippocampal axons in the mPFC (areas 24a, A25 and A32). Histogram shows comparison of bouton density between superficial (II-III, blue) and deep (V-VI, red) layers. Average, green. Vertical lines indicate SD.

Appositions between hippocampal projections with CB inhibitory neurons in the ACC

Viewing post-synaptic targets in areas 24a, 25 and 32 is needed to accurately characterize the pathway between the HPC and mPFC. Using labeling for inhibitory neurons for the calcium binding proteins CB, CR and PV, several stacks of images of appositions were captured, processed and analyzed (n = 4,636). Image J and Reconstruct were used to view the appositions. With regard to cortical inhibitory neurons, the superficial layers have a higher density of CB neurons, which synapse on dendrites of pyramidal neurons, and CR inhibitory neurons, which synapse with other inhibitory neurons (DeFelipe, 1997). PV positive inhibitory neurons are more prevalent in the deep layers, which synapse on the soma or proximal dendrites of excitatory pyramidal neurons (DeFelipe, 1997). Using a laser scanning confocal microscope for analysis, I discovered that projections to the deep layers of the mPFC formed appositions most frequently with PV neurons, followed by CB neurons. Table 4 displays the number of hippocampal axons apposed with dendritic elements labeled with each calcium binding protein, across all areas and cases. Table 5 further shows by layer, the small number of neurons recognized as inhibitory (8.8%). Figure 8A, shows examples of appositions between the hippocampal axon and a dendrite from a CB neuron at 10 μm (case BT-L).

Using Image J, appositions were viewed at a scale of 10 μm in 3D view. The 3D image was rotated 30 degrees on the y-axis four times in order to view the hippocampal axon bouton apposed with an inhibitory axon at different angles. White arrows show the location of the apposition for each image. Figure 8B, shows an apposition with a CR

neuron and a hippocampal axon (case BQ-L). Figure 8C shows another CB neuron closely apposed to a hippocampal axon (case BQ-L). Appositions shown in Figure 8 were found in the deep layers and superficial layers. Appositions, as indicated in Figure 9A, occurred most often in area 25 with CB neurons (3.6%), followed by CR neurons (2.6%) and lastly PV neurons (0.6%). In area 32, hippocampal axons were apposed with CB neurons more frequently (1.6%) than CR neurons (0.8%). Only a few PV neurons were apposed with hippocampal axons in area 32 (.04%). Appositions were more prevalent in area 25, while there was no evidence of appositions in area 24a in all cases.

Next I examined the hippocampal axons apposing calcium binding inhibitory neurons per cortical layer (n = 407), which accounted for 8.8% of all appositions with inhibitory neurons (Figure 9B). In the superficial layers (II-III) the prevalence of appositions between hippocampal axons and inhibitory neurons occurred most frequently with CB (50.3%). Within the superficial layers, hippocampal axons in layer III made appositions with a larger proportion of CB neurons (32.9%), whereas in layer II there were 17.4% appositions. Appositions between hippocampal axons and inhibitory neurons also occurred with CR (32.5%). In layer III there were more appositions with CR neurons (17.9%) compared to layer II (14.6%). In the deep layers (V-VI) the prevalence of appositions occurred most frequently with PV (8.1%). Within the deep layers, hippocampal axons in layer V made appositions with a larger proportion of PV neurons (6.9%), whereas in layer VI appositions were fewer (1.2%). Appositions between hippocampal axons and inhibitory neurons also occurred with elements of CB neurons (4.7%). Layer V included more appositions between HPC boutons and CB inhibitory

neurons (4.4%) compared to layer VI (.3%). Finally, appositions between HPC boutons with elements of CR neurons were present (3.7%), but no appositions were formed in layer VI.

Table 4: Hippocampal axons apposed to elements labeled for calcium binding proteins

	PV			CB			CR		
Case	A24a	A25	A32	A24a	A25	A32	A24a	A25	A32
RBQ (1563)*	0	9	2	0	48	7	0	31	18
RBS (163)*	0	4	1	0	20	8	0	16	12
RBT (2899)*	0	11	9	0	81	60	0	42	28
RBV (11)*	0	0	0	0	0	0	0	0	0
Totals	0	24	12	0	149	75	0	89	58

*Numerical values in parenthesis next to each case signifies the number of labeled boutons observed

Table 5: Hippocampal axons apposed to elements labeled for calcium binding proteins, by layer

	PV	CB	CR
Layer I	0	0	0
Layer II	2	71	59
Layer III	1	134	73
Layer V	28	18	15
Layer VI	5	1	0

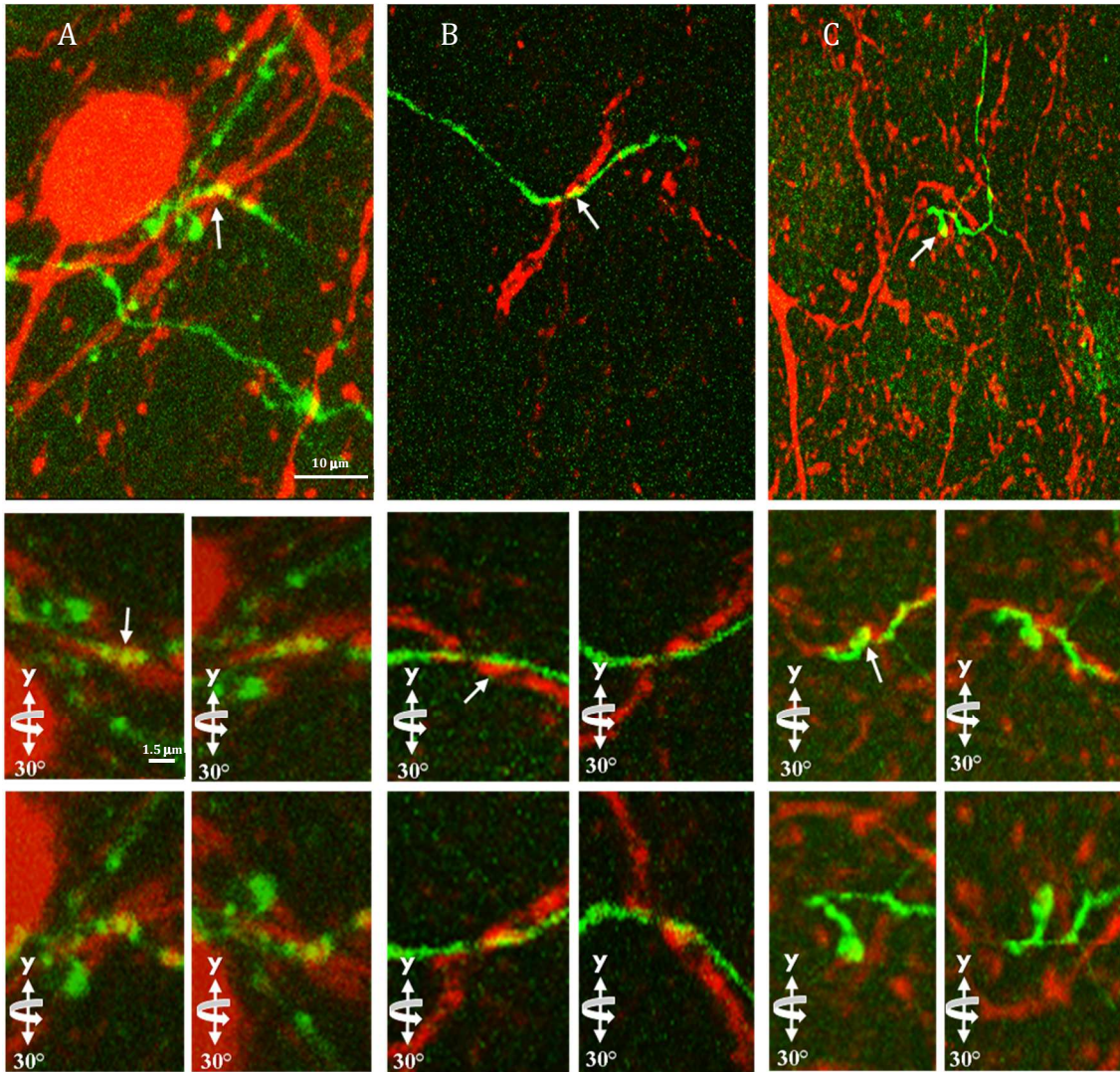


Figure 8: Examples of hippocampal axons apposed to elements of inhibitory neurons in the mPFC. *A*, Apposition shown (white arrows) in the deep layers of area 25 between a hippocampal axon (green) and a dendrite of a CB neuron (red) in case BT-L. Scale bar: 10 μm . Below, 3D images of apposition with 30° rotation on the y-axis. Scale bar: 1.5 μm . *B*, Apposition in the deep layers of area 32 between hippocampal axon (green) and dendrite of a CR neuron (red) in case BQ-L. Scale bar: 10 μm . Below, 3D images of apposition with 30° rotation on the y axis. Scale bar: 1.5 μm . *C*, Apposition in the deep layers of area 25 between hippocampal axon (green) and dendrite of a CB neuron (red) in case BQ-L. Scale bar: 10 μm . Below, 3D images of apposition with 30° rotation on the y axis. Scale bar: 1.5 μm .

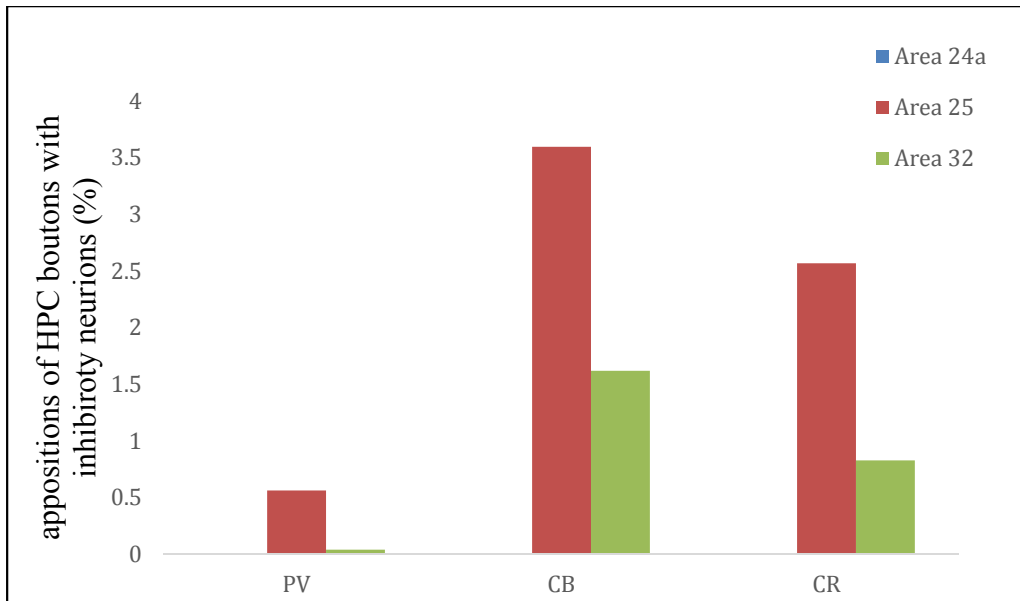


Figure 9: Areal pattern of hippocampal axons apposed to elements of inhibitory neurons in the ACC. Histogram shows that appositions were formed mostly between hippocampal axons and CB neurons in area 25 (red). No appositions were found in area 24a (blue). A32, green.

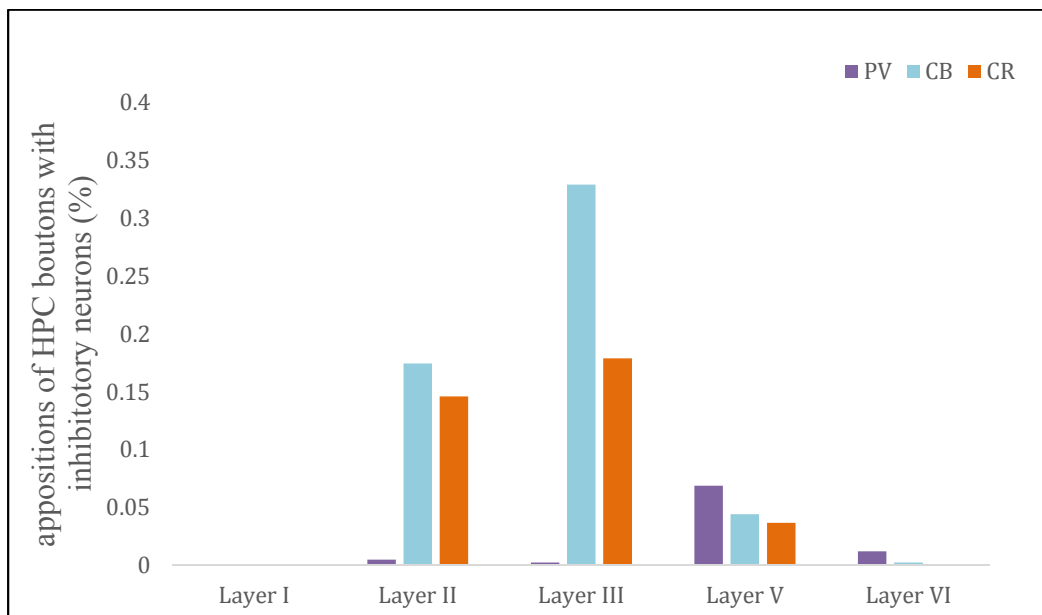


Figure 10: Laminar pattern of hippocampal axons apposed to elements of inhibitory neurons in the ACC. Hippocampal axons apposed to inhibitory neurons in the ACC (PV- purple, CB – blue, CR – orange).

Discussion

The results showed that the pathways from HPC preferentially terminate in area 25 of the mPFC. The pathway from HPC (CA1) had larger and more dense boutons in area 25 compared to areas 24a and 32 of the ACC and targeted some neurons belonging to the neurochemical class of CB inhibitory neurons. Results based on several methods in my present research suggest that area 25 has a strong influence in the connection between the HPC and mPFC.

Hippocampal pathways preferentially target area 25 of the ACC

Axonal mapping of labeled hippocampal axons showed consistently dense innervation of area 25 of the ACC compared to areas 24a and 32, which also receive projections from the HPC (Barbas & Blatt, 1995; Barbas *et al.*, 2011). The robust axon distribution in anterior and posterior area 25 raises the possibility that area 25 plays a bigger role in mnemonic processes in comparison to the other areas of the ACC.

Previous studies indicate that neurons involved in mnemonic activity are more prevalent in posterior than anterior HPC (Carmichael & Price, 1995). However, more robust connections to the PFC originate from the anterior HPC in comparison to the posterior part of the HPC (Barbas & Blatt, 1995; Carmichael & Price, 1995). These findings correlate with studies that reveal CA1 of the HPC as having more dense projections to the mPFC (Barbas & Blatt, 1995; Zhong *et al.*, 2006).

Density of pathway terminations in ACC is highest in area 25

Unbiased stereology conducted for the hippocampal pathways to areas 24a, 25 and 32, also revealed that area 25 had the highest density of boutons. The density of terminations in the pathway from the HPC to area 25 may indicate its relative strength compared to areas 24a and 32. Area 25 also included boutons with the largest diameters, which suggests a larger number of mitochondria and synaptic vesicles. With the highest density of boutons in area 25, compared to areas 24a and 32, this further illustrates a more efficient transmission system. Evidence suggests that area 25 plays a major role in the HPC-mPFC pathway, and possibly in memory processing.

Classifying boutons by major diameter revealed that hippocampal axons in area 25 had the largest distribution of boutons amongst the small and large bouton clusters (cluster cutoff size = $.8 \mu\text{m}$). Previous studies revealed that mitochondria number directly correlates with the labeled bouton volume, so it can be assumed that larger boutons would contain more mitochondria. It was discovered that smaller boutons may lack mitochondria (Germuska *et al.*, 2006). Furthermore, bouton size can be correlated with vesicle numbers. Larger boutons have more vesicles and are present in highly active pathways (Germuska *et al.*, 2006). Large boutons indicate that more vesicles have the potential to be released, which can lead to higher efficiency to transmit an impulse to the target (Zikopoulos & Barbas, 2007b). Thus, large boutons in area 25 may also have a larger quantity of synaptic vesicles and may display increased effectiveness in the HPC-mPFC pathway.

Studies also indicate that there is a consistent increase of bouton size from the superficial layers to deep layers (Germuska *et al.*, 2006; Medalla *et al.*, 2007). Figure 3B-C shows that the pathway from the HPC to areas 24a, 25 and 32 is consistent with previous findings. Studies at high resolution are needed to fully address this issue.

Hippocampal axons terminating in area 25 target superficial layers

Hippocampal axons projecting to the mPFC displayed distinct laminar patterns using several methods in the present study. Results showed that hippocampal axons had no preferential target between the superficial and deep layers in area 24a and area 32. However, in area 25, a laminar pattern of the distribution of hippocampal axons was seen in an anterior to posterior gradient. Posterior sections showed that axons preferentially targeted the deep layers (V-VI). The present study showed a larger distribution in layer V of the deep layers, in one case (BT-L, Figure 1B) and a larger distribution in layer VI (BQ-L, Figure 2B). More anterior sections showed that axons targeting the superficial layers (II-III) had a larger distribution in layer III in both cases (Figure 1B, 2B).

Studies focused on sensory areas showed that primary areas have a tendency to innervate the middle layers of sensory association areas while originating in layer III. This pathway could be defined as feedforward. Feedback pathways innervate the superficial layers, specifically layer I, and originate in the deep layers (Felleman & Van Essen, 1991). Feedforward refers to a pathway beginning at an area with more intricate lamination, which terminate in a less intricate area. Feedback refers to pathways with the opposite pattern (Barbas & Rempel-Clower, 1997). The present results distinguish the

connection from the HPC to mPFC as feedback projections. Indeed, the HPC has less elaborate lamination and projects to a cortical region that has more elaborate laminar structure. However, to explain the anterior-posterior gradient, I suggest that the more posterior mPFC resembles a feedforward system while the anterior mPFC resembles a feedback system. Perhaps, the HPC sends different signals regarding memory to the posterior mPFC compared to what is sent to the anterior mPFC. As present findings showed that area 25 displayed this gradient, anterior and posterior area 25 may play distinct roles in memory processing. Further research is needed to characterize the potential pathway between the HPC to anterior area 25 and posterior area 25.

ACC shows a progressive increase in bouton size from superficial to deep layers

Previous studies have shown that there is a consistent increase of bouton size from the superficial layers to deep layers (Germuska *et al.*, 2006; Medalla *et al.*, 2007). Analysis of bouton diameter in the present research is consistent with these findings. Bouton diameters were larger in the deep layers compared to the superficial layers across all areas of interest in the mPFC. Cluster analysis allowed for an in depth look at the laminar differences of the superficial and deep layers. Small clusters ($< .8\mu\text{m}$) did not show a major difference in diameter among areas 24a, 25 and 32, however the major laminar differences were seen in the large cluster ($\geq .8\mu\text{m}$). The overall distribution of boutons with larger diameters was greater in the deep layers compared to the superficial layers. While area 25 had the biggest laminar difference, this trend was seen with area 24a and area 32 as well. The significance of this trend is based on studies that show large

boutons having more vesicles, (Germuska *et al.*, 2006; Zikopoulos & Barbas, 2007b) and therefore the potential for neurotransmitter release (Tong & Jahr, 1994; Murthy *et al.*, 1997).

Hippocampal axons terminated most frequently in the superficial layers of the ACC

Quantitative analysis was conducted using unbiased stereology. This method revealed that the superficial layers had the highest bouton density compared to the deep layers. A previous study showed that HPC pathways preferentially terminate in layer III but also project to other cortical layers in the mPFC (Aggleton *et al.*, 2015), and the present findings are consistent with the previous data.

Studies have shown that termination patterns in cortical layers can be related to the laminar distinction between the origin and termination site of the projection (Barbas & Rempel-Clower, 1997). Present findings revealed that layer I had very few boutons (less than .003 percent) consistently across all cases and areas. Previous studies have shown that in comparison to eulaminate areas (areas with six layers), limbic areas have low density of neurons overall, and specifically in the superficial layers (Barbas & Pandya, 1989). Studies have discussed that neurons in limbic areas may have shorter developmental stages (Dombrowski *et al.*, 2001). As areas 24a, 25 and 32 are limbic areas, we can assume that they follow this trend. Deep layers in the cortex develop first and the superficial layers develop later, with layer I being the exception as being present first (Dombrowski *et al.*, 2001). There is no clear answer as to why layer I lacked labeled

boutons. Further research is needed, but the inside-out development of the cortex may help explain differences in density of connections (Sidman & Rakic, 1973).

Hippocampal axons preferentially target CB inhibitory neurons in the superficial layers

In primate cerebral cortex, inhibitory neurons can be grouped into non-overlapping neurochemical classes, which can be indicated by the expression of the calcium binding proteins CB, CR and PV (DeFelipe, 1997). PV has been shown to label inhibitory neurons that preferentially innervate excitatory pyramidal neurons at their proximal dendrites, axon initial segments or soma (DeFelipe *et al.*, 1989b). With fast-firing tendencies, PV neurons likely have strong inhibitory effects on pyramidal neurons (Constantinidis & Goldman-Rakic, 2002). CB labels inhibitory neurons that innervate the distal dendrites of pyramidal neurons and are non-fast spiking (DeFelipe *et al.*, 1989a; Kawaguchi & Kubota, 1997). Finally CR labels inhibitory neurons, which innervate other inhibitory neurons (DeFelipe *et al.*, 1989a).

Cortical inhibitory neurons in the superficial layers have the highest density of CB and CR, whereas the deep layers have a higher prevalence of PV inhibitory neurons. This method has become a convenient way to label inhibitory neurons in primates. When labeling inhibitory neurons for CB, CR and PV, the present findings allowed for the study of the post-synaptic targets of hippocampal pathways in area 24a, 25 and 32. Amongst a small number of synapses recognized as inhibitory (8.8%), the HPC innervated mostly CB and CR in the mPFC, specifically in area 25. The superficial and deep layers had the

highest prevalence of appositions in layer III and layer V, respectively. The HPC-mPFC pathway may thus have mostly excitatory effects but also inhibitory effects when hippocampal axons innervate inhibitory neurons in the mPFC.

Robust projections from the HPC to area 25 of the ACC may play a large role in memory

Animal lesion studies involving memory began to provide an understanding of which cortical structures may be involved in memory processing (Squire & Zola-Morgan, 1991). Studies on non-human primates have been conducted by lesioning certain cortical structures to study how it affects memory (Squire & Zola-Morgan, 1991). Memory could not be viewed as a unitary process, and it was discovered to involve multiple structures and pathways (Squire & Zola-Morgan, 1991). The HPC and mPFC have both been linked to memory processing in both rodents and primates (Amaral & Witter, 1989; Barbas & Blatt, 1995; Laroche *et al.*, 2000; Thierry *et al.*, 2000; Insausti & Munoz, 2001; Aggleton *et al.*, 2015).

Working memory refers to the ability to use relevant information/memories for a task and episodic memory refers to past personal events or experiences that include contextual details of those events (Jin & Maren, 2015). Working memory and episodic memory are constantly used in tandem. For example, when cooking a meal, information and memories of past experiences learning the recipe are used directly for the present task at hand. The mPFC has been shown to retrieve information from the HPC and relevant memories for the task at hand (Preston & Eichenbaum, 2013). The HPC and mPFC

synchronize in rhythmic activity during working and episodic memory, providing a clear picture that the connection is important in memory processing (Jones & Wilson, 2005).

Studies have shown that information flows from the HPC to the mPFC because hippocampal theta spikes first when in synchrony with the mPFC (Siapas *et al.*, 2005). Bilateral lesions to the HPC or mPFC impair memory in specific tasks and thus made it apparent that both structures are important in mnemonic processing. However, unilateral lesions to the HPC and mPFC kept memory intact, which reveals that an ipsilateral connection is sufficient for memory (Eichenbaum, 2017).

The present findings revealed that hippocampal axons robustly terminated in the mPFC, specifically area 25. Thus, among the connections between all areas of interest in the mPFC, area 25 can be assumed to have the strongest connection to the HPC and therefore, may be the most imperative in memory processing.

HPC-mPFC pathway implication in neurodegenerative diseases and psychiatric disorders

Alzheimer's disease

Alzheimer's disease (AD) is a complex neurodegenerative disease that affects cognition and memory (Mu & Gage, 2011). Studies have shown that AD affects the entorhinal cortex (Insausti & Munoz, 2001). The pathology of the disease then progresses and directly affects the CA1 of the HPC. As AD is a disease associated with aging in humans, a decline in neurogenesis has been studied as a cause for memory and cognitive

impairments (Clelland *et al.*, 2009). Thus, an increase in neurogenesis is believed to have a positive effect on this disease.

Tau is a protein that facilitates axonal transport by keeping the microtubules stable. Neurofibrillary tangles (NFTs) are aggregates of misfolded tau protein that are primary markers of AD (Mu & Gage, 2011; Serrano-Pozo *et al.*, 2011). As AD progresses, the HPC atrophies due to the presence of tau protein (Mu & Gage, 2011). Once atrophied, connections to and from the HPC are affected. The present findings show robust signal from the HPC to mPFC, which plays a role in memory. Therefore if damage occurs to the HPC due to AD, memory processing will be affected as well. Further understanding of the HPC-mPFC connection could lead to future understanding of AD.

Schizophrenia

The HPC-mPFC pathway plays a distinct role in cognition and memory and has been linked to several psychiatric disorders. Schizophrenia can be linked to cognitive impairment and abnormalities in the PFC. Studies have shown that schizophrenia decreases the integrity of the white matter in the ACC and HPC (Sigurdsson *et al.*, 2010). More severe symptoms occur if lesions involve the anterior HPC (Godsil *et al.*, 2013). Human studies and animal models of schizophrenia have shown that the mPFC and HPC show impaired memory processing as well as reduction in synchronization in the HPC-mPFC pathway (Sigurdsson *et al.*, 2010). One of the hippocampal structures targeted in

the pathology of schizophrenia is CA1 (Insausti & Munoz, 2001), which sends strong projections to mPFC (Barbas & Blatt, 1995), and shown further in this study.

Post-traumatic stress disorder (PTSD)

Traumatic memories experienced by post-traumatic stress disorder patients and animal models have also been linked to abnormal HPC-mPFC functioning (Liberzon & Sripada, 2008; Jin & Maren, 2015). Patients suffering with post-traumatic stress disorder display smaller ACC and hippocampal size (Karl *et al.*, 2006). Continued stress over long periods of time can weaken the connection between the HPC and mPFC (Admon *et al.*, 2009; Godsil *et al.*, 2013). Evidence also shows that PTSD patients show abnormal activity in the mPFC and HPC during fear conditioning tasks (Liberzon & Sripada, 2008). Linked to both fear tasks and memory, the HPC-mPFC cortex can be directly linked to post-traumatic stress disorder and studied for future therapeutic interventions.

Summary of findings and future direction

Several pieces of converging evidence indicate that the HPC sends robust signals to the mPFC. The HPC is an important structure involved in selecting and organizing relevant information and memories for a task at hand. The mPFC is needed for retrieving contextual memories. Through multiple methods, such as axon mapping, bouton diameter analysis, stereological methods for bouton distribution and density and appositions with inhibitory neurons, area 25 appears to have a major role in the HPC-mPFC connection. Further research is needed to characterize the potential pathway between the HPC to

anterior area 25 and posterior area 25. Research can be conducted to characterize this pathway post-synaptically with electron microscopy to investigate the inhibitory and excitatory targets of the hippocampal axons at the synaptic level. Further knowledge of the post-synaptic targets may reveal characteristics of the HPC-mPFC that may have implications for the causes of diseases affecting memory and emotions, needed to develop interventions for neurological and psychiatric diseases.

REFERENCES

- Admon, R., Lubin, G., Stern, O., Rosenberg, K., Sela, L., Ben-Ami, H. & Hendler, T. (2009) Human vulnerability to stress depends on amygdala's predisposition and hippocampal plasticity. *Proceedings of the National Academy of Sciences of the United States of America*, **106**, 14120–14125.
- Aggleton, J.P. & Brown, M.W. (1999) Episodic memory, amnesia, and the hippocampal-anterior thalamic axis. *Behavioral and Brain Sciences*, **22**, 425–444.
- Aggleton, J.P., Wright, N.F., Rosene, D.L. & Saunders, R.C. (2015) Complementary Patterns of Direct Amygdala and Hippocampal Projections to the Macaque Prefrontal Cortex. *Cerebral Cortex*, **25**(11), 4351–4373.
- Amaral, D.G. (1993) Emerging principles of intrinsic hippocampal organization. *Current Opinion in Neurobiology*, **2**, 225–229.
- Amaral, D.G. & Price, J.L. (1984) Amygdalo-cortical projections in the monkey (*Macaca fascicularis*) *Journal of Comparative Neurology*, **230**, 465–496.
- Amaral, D.G., Scharfman, H.E. & Lavenex, P. (2007) The dentate gyrus: fundamental neuroanatomical organization (dentate gyrus for dummies). *Progress in Brain Research*, **163**, 3–22.
- Amaral, D.G. & Witter, M.P. (1989) The three-dimensional organization of the hippocampal formation: a review of anatomical data. *Neuroscience*, **31**, 571–591.
- Anacker, C. & Hen, R. (2017) Adult hippocampal neurogenesis and cognitive flexibility - linking memory and mood. *Nature Reviews. Neuroscience*, **18**, 335–346.
- Barbas, H. (1995) Anatomic basis of cognitive-emotional interactions in the primate prefrontal cortex. *Neuroscience and Biobehavioral Reviews*, **19**, 499–510.
- Barbas, H. (2015) General Cortical and special Prefrontal Connections: Principles from Structure to Function. *Annual Review of Neuroscience*, **38**, 269–289.
- Barbas, H. & Blatt, G.J. (1995) Topographically specific hippocampal projections target functionally distinct prefrontal areas in the rhesus monkey. *Hippocampus*, **5**, 511–533.

- Barbas, H., Bunce, J.G. & Medalla, M. (2013) Prefrontal pathways that control attention. In Stuss, D.T., Knight, R. (eds) *Principles of frontal lobe functions*. Oxford University Press, New York (NY), pp. 31–48.
- Barbas, H. & De Olmos, J. (1990) Projections from the amygdala to basoventral and mediodorsal prefrontal regions in the rhesus monkey. *Journal of Comparative Neurology* **300**, 549–571.
- Barbas, H., Ghashghaei, H., Dombrowski, S.M. & Rempel-Clower, N.L. (1999) Medial prefrontal cortices are unified by common connections with superior temporal cortices and distinguished by input from memory-related areas in the rhesus monkey. *Journal of Comparative Neurology*, **410**, 343–367.
- Barbas, H. & Pandya, D.N. (1989) Architecture and intrinsic connections of the prefrontal cortex in the rhesus monkey. *Journal of Comparative Neurology*, **286**, 353–375.
- Barbas, H. & Rempel-Clower, N. (1997) Cortical structure predicts the pattern of corticocortical connections. *Cerebral Cortex*, **7**, 635–646.
- Barbas, H. & Zikopoulos, B. (2006) Sequential and parallel circuits for emotional processing in primate orbitofrontal cortex. In David, Z., Scott, R. (eds.) *The Orbitofrontal Cortex*. Oxford University Press, Oxford, pp. 57–91.
- Barbas, H., Zikopoulos, B. & Timbie, C. (2011) Sensory Pathways and Emotional Context for Action in Primate Prefrontal Cortex. *Biological Psychiatry*, **69**, 1133–1139.
- Blatt, G.J. & Rosene, D.L. (1998) Organization of direct hippocampal efferent projections to the cerebral cortex of the rhesus monkey: projections from CA1, prosubiculum, and subiculum to the temporal lobe. *Journal of Comparative Neurology*, **392**, 92–114.
- Burwell, R.D. & Amaral, D.G. (1998) Perirhinal and postrhinal cortices of the rat: interconnectivity and connections with the entorhinal cortex. *Journal of Comparative Neurology*, **391**, 293–321.
- Carmichael, S.T. & Price, J.L. (1995) Sensory and premotor connections of the orbital and medial prefrontal cortex of macaque monkeys. *Journal of Comparative Neurology*, **363**, 642–664.
- Cassel, J.C., Pereira de Vasconcelos, A., Loureiro, M., Cholvin, T., Dalrymple-Alford, J.C. & Vertes, R.P. (2013) The reuniens and rhomboid nuclei: neuroanatomy, electrophysiological characteristics and behavioral implications. *Progress in Neurobiology*, **111**, 34–52.

- Cenquizca, L.A. & Swanson, L.W. (2007) Spatial organization of direct hippocampal field CA1 axonal projections to the rest of the cerebral cortex. *Brain Research. Brain Research Reviews*, **56**, 1–26.
- Churchwell, J.C. & Kesner, R.P. (2011) Hippocampal-prefrontal dynamics in spatial working memory: interactions and independent parallel processing. *Behavioural Brain Research*, **225**, 389–395.
- Clelland, C.D., Choi, M., Romberg, C., Clemenson, G.D., Jr., Fragniere, A., Tyers, P., Jessberger, S., Saksida, L.M., Barker, R.A., Gage, F.H. & Bussey, T.J. (2009) A functional role for adult hippocampal neurogenesis in spatial pattern separation. *Science*, **325**, 210–213.
- Constantinidis, C. & Goldman-Rakic, P.S. (2002) Correlated discharges among putative pyramidal neurons and interneurons in the primate prefrontal cortex. *Journal of Neurophysiology*, **88**, 3487–3497.
- Corcoran, K.A. & Quirk, G.J. (2007) Activity in prelimbic cortex is necessary for the expression of learned, but not innate, fears. *Journal of Neuroscience*, **27**, 840–844.
- DeFelipe, J. (1997) Types of neurons, synaptic connections and chemical characteristics of cells immunoreactive for calbindin-D28K, parvalbumin and calretinin in the neocortex. *Journal of Chemical Neuroanatomy*, **14**, 1–19.
- DeFelipe, J., Hendry, S.H. & Jones, E.G. (1989a) Synapses of double bouquet cells in monkey cerebral cortex visualized by calbindin immunoreactivity. *Brain Research*, **503**, 49–54.
- DeFelipe, J., Hendry, S.H. & Jones, E.G. (1989b) Visualization of chandelier cell axons by parvalbumin immunoreactivity in monkey cerebral cortex. *Proceedings of the National Academy of Sciences of the United States of America*, **86**, 2093–2097.
- Dolleman-Van der Weel, M.J., Lopes da Silva, F.H. & Witter, M.P. (1997) Nucleus Reunions Thalami Modulates Activity in Hippocampal Field CA1 through Excitatory and Inhibitory Mechanisms. *Journal of Neuroscience*, **17**, 5640–5650.
- Dombrowski, S.M., Hilgetag, C.C. & Barbas, H. (2001) Quantitative architecture distinguishes prefrontal cortical systems in the rhesus monkey. *Cerebral Cortex*, **11**, 975–988.
- Eichenbaum, H. (2017) Prefrontal-hippocampal interactions in episodic memory. *Nature Reviews. Neuroscience*, **18**, 547–558.

- Felleman, D.J. & Van Essen, D.C. (1991) Distributed hierarchical processing in the primate cerebral cortex. *Cerebral Cortex*, **1**, 1–47.
- Fiala, J.C. (2005) Reconstruct: a free editor for serial section microscopy. *Journal of Microscopy*, **218**, 52–61.
- Floresco, S.B., Seamans, J.K. & Phillips, A.G. (1997) Selective roles for hippocampal, prefrontal cortical, and ventral striatal circuits in radial-arm maze tasks with or without a delay. *Journal of Neuroscience*, **17**, 1880–1890.
- Frerking, M. & Wilson, M. (1996) Saturation of postsynaptic receptors at central synapses? *Current Opinion in Neurobiology*, **6**, 395–403.
- García-Cabezas, M.A. & Barbas, H. (2017) Anterior Cingulate Pathways May Affect Emotions Through Orbitofrontal Cortex. *Cerebral Cortex*, **27**(10), 4891–4910. doi:10.1093/cercor/bhw284.
- Germuska, M., Saha, S., Fiala, J. & Barbas, H. (2006) Synaptic distinction of laminar-specific prefrontal-temporal pathways in primates. *Cerebral Cortex*, **16**, 865–875.
- Ghashghaei, H.T., Hilgetag, C.C. & Barbas, H. (2007) Sequence of information processing for emotions based on the anatomic dialogue between prefrontal cortex and amygdala. *NeuroImage*, **34**, 905–923.
- Giustino, T.F. & Maren, S. (2015) The Role of the Medial Prefrontal Cortex in the Conditioning and Extinction of Fear. *Frontiers in Behavioral Neuroscience*, **9**, 298.
- Glaser, E.M. & Wilson, P.D. (1998) The coefficient of error of optical fractionator population size estimates: a computer simulation comparing three estimators. *Journal of Microscopy*, **192**, 163–171.
- Godsil, B.P., Kiss, J.P., Spedding, M. & Jay, T.M. (2013) The hippocampal-prefrontal pathway: the weak link in psychiatric disorders? *European Neuropsychopharmacology*, **23**, 1165–1181.
- Gomez-Isla, T., Price, J.L., McKeel, D.W., Morris, J.C., Growdon, J.H. & Hyman, B.T. (1996) Profound loss of layer II entorhinal cortex neurons occurs in very mild Alzheimer's disease. *Journal of Neuroscience*, **16**, 4491–4500.
- Gundersen, H.J., Jensen, E.B., Kieu, K. & Nielsen, J. (1999) The efficiency of systematic sampling in stereology--reconsidered. *Journal of Microscopy*, **193**, 199–211.
- Hasselmo, M.E. & Eichenbaum, H. (2005) Hippocampal mechanisms for the context-dependent retrieval of episodes. *Neural Networks*, **18**, 1172–1190.

- Hembrook, J.R., Onos, K.D. & Mair, R.G. (2012) Inactivation of ventral midline thalamus produces selective spatial delayed conditional discrimination impairment in the rat. *Hippocampus*, **22**, 853–860.
- Henson, R.N., Shallice, T. & Dolan, R.J. (1999) Right prefrontal cortex and episodic memory retrieval: a functional MRI test of the monitoring hypothesis. *Brain*, **122**, 1367–1381.
- Howard, M.W., Fotedar, M.S., Datey, A.V. & Hasselmo, M.E. (2005) The temporal context model in spatial navigation and relational learning: toward a common explanation of medial temporal lobe function across domains. *Psychological Review*, **112**, 75–116.
- Igarashi, K.M., Lu, L., Colgin, L.L., Moser, M.B. & Moser, E.I. (2014) Coordination of entorhinal-hippocampal ensemble activity during associative learning. *Nature*, **510**, 143–147.
- Insausti, R. & Amaral, D.G. (2008) Entorhinal cortex of the monkey: IV. Topographical and laminar organization of cortical afferents. *Journal of Comparative Neurology*, **509**, 608–641.
- Insausti, R., Amaral, D.G. & Cowan, W.M. (1987) The entorhinal cortex of the monkey: III. Subcortical afferents. *Journal of Comparative Neurology*, **264**, 396–408.
- Insausti, R. & Munoz, M. (2001) Cortical projections of the non-entorhinal hippocampal formation in the cynomolgus monkey (*Macaca fascicularis*). *European Journal of Neuroscience*, **14**, 435–451.
- Jay, T.M. & Witter, M.P. (1991) Distribution of hippocampal CA1 and subicular efferents in the prefrontal cortex of the rat studied by means of anterograde transport of Phaseolus vulgaris-leucoagglutinin. *Journal of Comparative Neurology*, **313**, 574–586.
- Jin, J. & Maren, S. (2015) Prefrontal-Hippocampal Interactions in Memory and Emotion. *Frontiers in Systems Neuroscience*, **9**, 170.
- Jones, M.W. & Wilson, M.A. (2005) Theta rhythms coordinate hippocampal-prefrontal interactions in a spatial memory task. *PLoS Biology*, **3**, e402.
- Karl, A., Schaefer, M., Malta, L.S., Dorfel, D., Rohleder, N. & Werner, A. (2006) A meta-analysis of structural brain abnormalities in PTSD. *Neuroscience and Biobehavioral Reviews*, **30**, 1004–1031.
- Kawaguchi, Y. & Kubota, Y. (1997) GABAergic cell subtypes and their synaptic connections in rat frontal cortex. *Cerebral Cortex*, **7**, 476–486.

- Keene, C.S., Bladon, J., McKenzie, S., Liu, C.D., O'Keefe, J. & Eichenbaum, H. (2016) Complementary Functional Organization of Neuronal Activity Patterns in the Perirhinal, Lateral Entorhinal, and Medial Entorhinal Cortices. *Journal of Neuroscience*, **36**, 3660–3675.
- Kennedy, P.J. & Shapiro, M.L. (2004) Retrieving memories via internal context requires the hippocampus. *Journal of Neuroscience*, **24**, 6979–6985.
- Laroche, S., Davis, S. & Jay, T.M. (2000) Plasticity at hippocampal to prefrontal cortex synapses: dual roles in working memory and consolidation. *Hippocampus*, **10**, 438–446.
- Liberzon, I. & Sripada, C.S. (2008) The functional neuroanatomy of PTSD: a critical review. *Progress in Brain Research*, **167**, 151–169.
- Medalla, M., Lera, P., Feinberg, M. & Barbas, H. (2007) Specificity in inhibitory systems associated with prefrontal pathways to temporal cortex in primates. *Cerebral Cortex*, **17 Suppl 1**, i136–i150.
- Miller, E.K. & Cohen, J.D. (2001) An integrative theory of prefrontal cortex function. *Annual Review of Neuroscience*, **24**, 167–202.
- Mishkin, M. (1978) Memory in monkeys severely impaired by combined but not by separate removal of amygdala and hippocampus. *Nature*, **273**, 297–298.
- Mitchell, A.S., Sherman, S.M., Sommer, M.A., Mair, R.G., Vertes, R.P. & Chudasama, Y. (2014) Advances in understanding mechanisms of thalamic relays in cognition and behavior. *Journal of Neuroscience*, **34**, 15340–15346.
- Morecraft, R.J., Geula, C. & Mesulam, M.M. (1992) Cytoarchitecture and neural afferents of orbitofrontal cortex in the brain of the monkey. *Journal of Comparative Neurology*, **323**, 341–358.
- Morecraft, R.J. & Van Hoesen, G.W. (1992) Cingulate input to the primary and supplementary motor cortices in the rhesus monkey: evidence for somatotopy in areas 24c and 23c. *Journal of Comparative Neurology*, **322**, 471–489.
- Mu, Y. & Gage, F.H. (2011) Adult hippocampal neurogenesis and its role in Alzheimer's disease. *Molecular Neurodegeneration*, **6**, 85.
- Murthy, V.N., Sejnowski, T.J. & Stevens, C.F. (1997) Heterogeneous release properties of visualized individual hippocampal synapses. *Neuron*, **18**, 599–612.

- Navawongse, R. & Eichenbaum, H. (2013) Distinct pathways for rule-based retrieval and spatial mapping of memory representations in hippocampal neurons. *Journal of Neuroscience*, **33**, 1002–1013.
- Ongur, D. & Price, J.L. (2000) The organization of networks within the orbital and medial prefrontal cortex of rats, monkeys and humans. *Cerebral Cortex*, **10**, 206–219.
- Orban, G.A., Van Essen, D. & Vanduffel, W. (2004) Comparative mapping of higher visual areas in monkeys and humans. *Trends in Cognitive Sciences*, **8**, 315–324.
- Penfield, W. & Milner, B. (1958) Memory deficit produced by bilateral lesions in the hippocampal zone. *A.M.A. Archives of Neurology and Psychiatry*, **79**, 475–497.
- Preston, A.R. & Eichenbaum, H. (2013) Interplay of hippocampus and prefrontal cortex in memory. *Current Biology*, **23**, R764–773.
- Ranganath, C., Heller, A., Cohen, M.X., Brozinsky, C.J. & Rissman, J. (2005) Functional connectivity with the hippocampus during successful memory formation. *Hippocampus*, **15**, 997–1005.
- Rosene, D.L. & Van Hoesen, G.W. (1977) Hippocampal efferents reach widespread areas of cerebral cortex and amygdala in the rhesus monkey. *Science*, **198**, 315–317.
- Rosene, D.L. & Van Hoesen, G.W. (1987) The hippocampal formation of the primate brain. A review of some comparative aspects of cytoarchitecture and connections. In Jones, E.G., Peters, A. (eds.) *Cerebral Cortex, Vol.6*. Plenum Publishing Corporation, New York, pp. 345–455.
- Rushworth, M.F., Noonan, M.P., Boorman, E.D., Walton, M.E. & Behrens, T.E. (2011) Frontal cortex and reward-guided learning and decision-making. *Neuron*, **70**, 1054–1069.
- Scoville, W.B. (1954) Orbital undercutting in the treatment of psychoneuroses, depressions and senile emotional states; psychiatric and physiologic results of fractional lobotomy in the milder emotional illnesses. *Diseases of the Nervous System*, **15**, 324–334.
- Scoville, W.B. & Milner, B. (1957) Loss of recent memory after bilateral hippocampal lesions. *Journal of Neurology, Neurosurgery, and Psychiatry*, **20**, 11–21.
- Serrano-Pozo, A., Frosch, M.P., Masliah, E. & Hyman, B.T. (2011) Neuropathological Alterations in Alzheimer Disease. *Cold Spring Harbor Perspectives in Biology*, **3**.

- Siapas, A.G., Lubenov, E.V. & Wilson, M.A. (2005) Prefrontal phase locking to hippocampal theta oscillations. *Neuron*, **46**, 141–151.
- Sidman, R.L. & Rakic, P. (1973) Neuronal migration, with special reference to developing human brain: a review. *Brain Research*, **62**, 1–35.
- Sigurdsson, T. & Duvarci, S. (2015) Hippocampal-Prefrontal Interactions in Cognition, Behavior and Psychiatric Disease. *Frontiers in Systems Neuroscience*, **9**, 190.
- Sigurdsson, T., Stark, K.L., Karayiorgou, M., Gogos, J.A. & Gordon, J.A. (2010) Impaired hippocampal-prefrontal synchrony in a genetic mouse model of schizophrenia. *Nature*, **464**, 763–767.
- Simons, J.S. & Spiers, H.J. (2003) Prefrontal and medial temporal lobe interactions in long-term memory. *Nature Reviews. Neuroscience*, **4**, 637–648.
- Sotres-Bayon, F., Sierra-Mercado, D., Pardilla-Delgado, E. & Quirk, G.J. (2012) Gating of fear in prelimbic cortex by hippocampal and amygdala inputs. *Neuron*, **76**, 804–812.
- Squire, L.R. (1992) Memory and the hippocampus: A synthesis from findings with rats, monkeys, and humans. *Psychological Reviews*, **99**, 195–231.
- Squire, L.R., Stark, C.E. & Clark, R.E. (2004) The medial temporal lobe. *Annual Review of Neuroscience*, **27**, 279–306.
- Squire, L.R. & Zola-Morgan, S. (1991) The medial temporal lobe memory system. *Science*, **253**, 1380–1386.
- Thierry, A.M., Gioanni, Y., Degenetais, E. & Glowinski, J. (2000) Hippocampo-prefrontal cortex pathway: anatomical and electrophysiological characteristics. *Hippocampus*, **10**, 411–419.
- Tierney, P.L., Degenetais, E., Thierry, A.M., Glowinski, J. & Gioanni, Y. (2004) Influence of the hippocampus on interneurons of the rat prefrontal cortex. *European Journal of Neuroscience*, **20**, 514–524.
- Tong, G. & Jahr, C.E. (1994) Multivesicular release from excitatory synapses of cultured hippocampal neurons. *Neuron*, **12**, 51–59.
- Tronel, S. & Sara, S.J. (2002) Mapping of olfactory memory circuits: region-specific c-fos activation after odor-reward associative learning or after its retrieval. *Learning & Memory*, **9**, 105–111.

- Van Hoesen, G.W., Pandya, D.N. & Butters, N. (1975) Some connections of the entorhinal (area 28) and perirhinal (area 35) cortices of the rhesus monkey. II. Frontal lobe afferents. *Brain Research*, **95**, 25–38.
- Vertes, R.P. (2006) Interactions among the medial prefrontal cortex, hippocampus and midline thalamus in emotional and cognitive processing in the rat. *Neuroscience*, **142**, 1–20.
- Vogt, B.A. & Pandya, D.N. (1987) Cingulate cortex of the rhesus monkey: II. Cortical afferents. *Journal of Comparative Neurology*, **262**, 271–289.
- Witter, M.P., Naber, P.A., van Haeften, T., Machielsen, W.C., Rombouts, S.A., Barkhof, F., Scheltens, P. & Lopes da Silva, F.H. (2000) Cortico-hippocampal communication by way of parallel parahippocampal-subicular pathways. *Hippocampus*, **10**, 398–410.
- Zhong, Y.M., Yukie, M. & Rockland, K.S. (2006) Distinctive morphology of hippocampal CA1 terminations in orbital and medial frontal cortex in macaque monkeys. *Experimental Brain Research*, **169**, 549–553.
- Zikopoulos, B. & Barbas, H. (2006) Prefrontal projections to the thalamic reticular nucleus form a unique circuit for attentional mechanisms. *Journal of Neuroscience*, **26**, 7348–7361.
- Zikopoulos, B. & Barbas, H. (2007a) Circuits for multisensory integration and attentional modulation through the prefrontal cortex and the thalamic reticular nucleus in primates. *Reviews in the Neurosciences*, **18** 417–438.
- Zikopoulos, B. & Barbas, H. (2007b) Parallel driving and modulatory pathways link the prefrontal cortex and thalamus *PLoS One*, **2**, e448.

VITA

